THE ASTRONOMICAL JOURNAL VOLUME 105, NUMBER 6 JUNE 1993

GRAVITATIONAL LENSING STATISTICS BASED ON A LARGE SAMPLE OF HIGHLY LUMINOUS QUASARS[1]

J. SURDEJ[2] AND J. F. CLAESKENS
Institut d'Astrophysique, Université de Liège, Avenue de Cointe 5, B-4000 Liège, Belgium
Electronic mail: surdej@astra.astro.ulg.ac.be., claeskens@astra.astro.ulg.ac.be

D. CRAMPTON
Dominion Astrophysical Observatory, 5071 West Saanich Road, Victoria, British Columbia V8X 4M6, Canada
Electronic mail: crampton@dao.nrc.ca

A. V. FILIPPENKO
Department of Astronomy, University of California, Berkeley, California 94720
Electronic mail: alex%avf.hepnet@lbl.bitnet

D. HUTSEMÉKERS AND P. MAGAIN[3]
Institut d'Astrophysique, Université de Liège, Avenue de Cointe 5, B-4000 Liège, Belgium
Electronic mail: hutsemek@astra.astro.ulg.ac.be, magain@astra.astro.ulg.ac.be

B. PIRENNE
ST-ECF, c/o ESO, Karl-Schwarzschild str. 2, D-8046 Garching bei München, Germany
Electronic mail: bpirenne@eso.org

C. VANDERRIEST
Observatoire de Meudon, DAEC, Place J. Janssen 5, F-92195 Meudon Principal Cédex, France
Electronic mail: vanderri@frmeu51.bitnet

H. K. C. YEE
Department of Astronomy, University of Toronto, Toronto, Ontario, Canada M5S 1A7
Electronic mail: hyee@utorphys.bitnet

Received 1992 May 15; revised 1992 December 21

ABSTRACT

Results on gravitational lensing statistics applied to a sample of 469 highly luminous quasars are reported. The objects were directly imaged, either from the ground (ESO, CFH) under optimal seeing conditions, or using the *Hubble Space Telescope*. We have derived values for the effectiveness parameter F of galaxies, modeled by means of singular isothermal spheres, to produce macrolensed images of distant quasars, and upper limits on the density parameter Ω_L of compact objects with masses $\simeq 10^{10}$–$10^{12} \mathcal{M}_\odot$. Adopting $H_0 = 50$ km/s/Mpc, $\Omega_0 = 1$ and $\Lambda = 0$, we find that at the 99.7% confidence level, $0.005 < F < 0.478$ and that $\Omega_L < 0.02$. A critical discussion of these results is presented. Finally, comparing the efficiencies of ground-based and space instruments used to search for gravitational lens systems among highly luminous quasars, we conclude that for the near future, ground based direct imaging characterized by a good dynamical range still constitutes the best observational strategy.

1. INTRODUCTION

Since macrogravitational lens systems provide us with equivalent optical benches having dimensions comparable to that of the Universe, we may conveniently use them in order to infer various parameters of astrophysical (mass of deflecting galaxies, size of intervening gas clouds, etc.) and cosmological (H_0, Ω_0, Λ, etc.) significance. We refer to Blandford & Narayan (1992) for a general review on this subject. The possibility of using statistical gravitational lens studies as an astrophysical or cosmological tool has motivated the present work. Indeed, following the theoretical work of Turner *et al.* (1984), dealing with a realistic determination of the optical depth for macrolensing, it was natural to expect that high angular resolution direct observations of a large sample of bright and distant quasars would constitute the best approach in searching for new lens candidates, and also in setting limits on various astrophysical and cosmological parameters. In the next section, we describe such a sample of 469 highly luminous quasars

[1]Based upon observations collected at the European Southern Observatory (La Silla, Chile), with the Canada France Hawaii Telescope and with the Hubble Space Telescope.
[2]Maître de Recherches au Fonds National de la Recherche Scientifique (Belgique) and visiting astronomer at ESO (Garching bei München, Germany).
[3]Chercheur Qualifié au Fonds National de la Recherche Scientifique (Belgique).

 0004-6256/93/062064-15$00.90

(hereafter HLQs) that have been observed either under good seeing conditions using ground based telescopes at ESO and CFH or with the Hubble Space Telescope (*HST*).

On the basis of the observed frequency of multiply lensed HLQ images detected in this sample, we present in Sec. 3 results on lensing statistics relevant to (i) the value of the effectiveness parameter F of galaxies to produce multiply lensed quasar images and to (ii) upper limits on the density parameter Ω_L of compact objects with masses $\simeq 10^{10}$–$10^{12} \mathscr{M}_\odot$. Similar statistical results have been recently reported for a sample of 215 quasars and another one of 184 quasars by Surdej *et al.* (1992b) and Maoz *et al.* (1992b), respectively.

A discussion as well as general conclusions form the last two sections of the present paper.

2. DESCRIPTION OF FOUR LARGE SAMPLES OF HIGHLY LUMINOUS QUASARS

Considering the canonical $\log(N)$–B relation for the number of quasars per unit area brighter than a given magnitude B (cf. Boyle *et al.* 1988), it is easy to calculate the number density enhancement of quasars $q(M,B_0)$ in a flux limited sample $B < B_0$ subject to a magnification M. Following Narayan (1989), one finds that $q(M,B_0) = N[< B_0 + 2.5 \log M]/(N[< B_0] \times M)$. Referring to Fig. 1 of Narayan (1989), where the author has illustrated the dependence of q on both M and B_0, one immediately sees that the magnification bias becomes more and more important as the limiting flux of the selected sample of quasistellar objects (QSOs) increases. We describe hereafter four major optical surveys for multiply lensed QSO images which benefit from this magnification bias. These QSO samples are subsequently used in Sec. 3 in the context of our statistical gravitational lens studies.

2.1 The ESO Key Programme Sample

Following the successful outcomes of the surveys for gravitational lens (GL) candidates among HLQs (typically $M_V \leqslant -27$ mag)[2] initiated in 1986 November by the Liège/ESO/Hamburg group (Surdej *et al.* 1988 a,b,c; Swings *et al.* 1990; Magain *et al.* 1990) and by Djorgovski & Meylan (1989a, b), an enlarged team of European and North American astronomers has been successful in obtaining observations at ESO in the framework of a Key Programme (Surdej *et al.* 1989, 1990, 1992a). Since 1989 May, the Danish 1.5 m (direct CCD camera), the ESO/MPI 2.2 m (direct CCD camera or EFOSC2), the 3.6 m (EFOSC1) and the NTT (EFOSC2, EMMI or SUSI) telescopes located at La Silla (Chile) have been used to study gravitational lensing effects. The first aim is to detect multiply lensed HLQs with typical angular separations smaller than one arcsec; furthermore, we are also looking for the presence of foreground galaxies in the vicinity of the relevant targets (cf. Van Drom 1992 and Van Drom *et al.* 1993 for a more detailed review) and even for the possible signs of a lensing galaxy whose image might be superimposed over that of the objects under study (Magain *et al.* 1992a; Van Drom *et al.* 1993). A full detailed account of the direct imagery observations obtained so far at ESO for 187 quasars selected from the Véron-Cetty & Véron (1987) catalogue may be found in Surdej *et al.* (1993). This latter compilation lists, for each HLQ observable from the southern hemisphere, its current identification, 1950 equatorial coordinates, redshift, apparent and absolute visual magnitudes (for the latter one, k-corrections were applied with $\alpha = -0.7$ and a magnitude correction for the presence of broad emission lines, see Véron-Cetty & Véron 1991), date of observation, filter and exposure time, seeing (FWHM), types of CCDs and telescopes used, the technique of image analysis that has been applied (direct visualization or point spread function PSF subtraction) and indications on whether the HLQ consists of a confirmed case of a GL (i.e., even if we are pessimistic, we are forced to recognize that it is a GL; for these cases we set $PQ=1$, otherwise $PQ=0$) or of just a possible candidate (we are here more optimistic but not totally certain that it is a GL and we set $OQ=1$, but $PQ=0$, for such candidates). In the latter cases, the distance θ_{DQ} (in arcsec) and the magnitude difference MQ between the identified secondary point source image and the primary one are also listed. Additional data related to the counts of galaxies near the quasars are also given. Part of this information is summarized in Table 3, which also contains similar data for the three other quasar samples described hereafter.

Accepted cases of gravitationally lensed quasars for which $PQ=1$ (and also of course $OQ=1$), identified in the ESO KP sample, have already been reported for the following objects: PG1115+080 (Weymann *et al.* 1980; this lens has been rediscovered in the course of our survey), UM673 (Surdej *et al.* 1987) and H1413+117 (Magain *et al.* 1988). Among the possible GL candidates appearing in the ESO KP sample and for which $OQ=1$ but $PQ=0$, let us mention UM425 (Meylan & Djorgovski 1989) and Q1208+1011 (Magain *et al.* 1992a,b; Maoz *et al.* 1992a; Bahcall *et al.* 1992b). There are, in fact, 18 GL candidates (i.e., with $OQ=1$ and $PQ=0$) for which more observations (direct imagery and/or spectroscopy) are required.

Because of the limited dynamical range ($\Delta m \simeq 5$ mag) of our direct CCD imaging and since galaxies alone are just capable of producing multiply lensed quasars with typical angular separations $\leqslant 3''$ (neglecting thus all possible effects due to clusters of galaxies), we only consider in the remainder those GL candidates for which $\theta_{DQ} \leqslant 3''$ and $MQ \leqslant 5$ mag. There remain 17 such candidates characterized by $OQ=1$. Furthermore, because we have been somewhat too generous when selecting optimistic candidates—in order not to lose potential GLs—we estimate that only half of the previous cases (i.e., in total $\simeq 3 + (17-3)/2 = 10$) actually consist of possible GL candidates.

[2]Unless quoted otherwise, we have adopted $H_0 = 50$ km/s/Mpc, $\Omega_0 = 1$ and $\Lambda = 0$.

2.2 The Crampton et al. Sample

Using an image stabilizing camera at the CFHT, Crampton *et al.* (1989) have also made a direct imaging search for closely spaced gravitationally lensed QSO components. The full width at half-maximum intensity (FWHM) of images produced by this camera is found to be typically 10%–20% better than for images recorded with a standard prime focus camera. Out of 32 quasars with $z > 1.6$ and $m_V < 19$ mag (i.e., $M_V < -26$ mag), seven were found to be possible GL candidates, two of these having subarcsec angular separations. This fraction (22%) of interesting HLQs is essentially the same as the one (23%) initially reported by Surdej *et al.* (1988c) for the Liège/ESO/Hamburg sample. Crampton *et al.* (1992) have extended their initial survey for lensed quasars to a total sample of 101 HLQs (see Table 3) located north of the equator and extracted from the Véron-Cetty & Véron (1987) catalogue. Crampton and his collaborators find three quasars for which the residual image remaining after subtraction of the appropriate PSF shows some evidence for additional image(s) with subarcsec separations. In addition, they report 11 quasars which have companion point sources with separations ranging between $\simeq 1''$ and $6''$. For five of these cases (PKS 0504+03, PG 1715+535, 17449 +206, PKS 1756+237 and 2203+29), the companion turns out to be a star. The companion to 4C56.28 has a redder color than the quasar (Crampton *et al.* 1989) but we still consider it as a possible GL candidate. There remain six GL candidates for which $OQ=1$, plus the three above with subarcsec separations.

Imposing also here the constraints $\theta_{DQ} \leqslant 3''$ and $MQ \leqslant 5$ mag, we are left with just four GL candidates for which $OQ=1$. Again, we estimate that only about half (i.e., $\simeq 2$) of these objects constitute possible lens candidates. Additional observations are absolutely mandatory in order to definitely identify their true nature (either $OQ=0$ or $PQ=1$). Let us further note that Crampton *et al.* (1992) report 18 cases of quasars which have nonstellar companions within $6''$. Therefore, out of 101 observed HLQs, they still identify a significant fraction ($\simeq 32\%$) of potentially interesting objects.

2.3 The Yee et al. Sample

Yee *et al.* (1993) report on direct imagery of 104 HLQs obtained in the Gunn r filter with the direct prime focus camera of the CFH telescope (see Table 3). Most of their observations are complementary to those carried out by Crampton *et al.* (1992). Yee *et al.* (1993) have rediscovered the gravitational lens H1413+117 (Magain *et al.* 1988) and the binary quasar PHL1222 (Djorgovski *et al.* 1987). Whenever a possible GL candidate was found at the telescope, additional multiband images were obtained. Several possible GL candidates with separation greater than $\simeq 1''$ (including PG 1715+535 and others) have been ruled out this way. For some candidates, spectroscopy has been obtained at Lick Observatory revealing that the close companions are stars. To test for closely-spaced GLs ($\leqslant 1''$), contour plots of the quasars were compared with reference stars in the field. No such candidates were found. The limits for detection of closely-spaced GLs were derived by simulations. This was done by testing the visibility of artificially added starlike companions with various magnitude differences and at different angular separations (see Yee *et al.* 1993 for a more detailed account).

2.4 The HST Snapshot Sample

A search for gravitationally lensed quasars using the *Hubble Space Telescope's* Planetary Camera, known as the *HST* nonproprietary snapshot survey (Bahcall *et al.* 1992a), was initiated in 1990 September. It consists in obtaining equivalent V and some I direct images (2 or 4 min and later 260 s exposures, image scale of 0.043″/pixel, 4 fields of $34'' \times 34''$), with an angular resolution $\simeq 0.1''$, of 354 high luminosity quasars ($z > 1$, $M_V < -25.5$ mag) (calculated for $H_0=100$ km/s/Mpc, $q_0=0.5$, $\alpha=-0.5$ + galactic correction, $|b| > 10°$), selected from the catalogue of Véron-Cetty & Véron (1987), during gaps in the *HST* scheduled observing program. To save time, most of the images are taken using only the gyroscopes for pointing and guiding. Despite the well-known spherical aberration of *HST*, the existing point spread function still permits the detection of nearby pointlike objects with separations of the order of several tenths of an arcsec. Until the end of 1991 March, useful high-resolution images had been obtained for 32 quasars. Each of these quasar exposures has been examined by eye for evidence of multiple images, the results being calibrated by simulations (Bahcall *et al.* 1992a). These authors report no evidence of multiple images due to gravitational lensing for these 32 objects. Maoz *et al.* (1992b) have recently published an additional list of 152 HLQs observed with *HST*, bringing their total number to 184 quasars. So far, they have only identified one GL candidate, namely the high redshift quasar Q1208+1011 (Maoz *et al.* 1992a), originally detected from the ground by Magain *et al.* (1992a) (see also Magain *et al.* 1992b and Pirenne *et al.* 1992). Maoz *et al.* (1992b) identified six other quasars having point sources within $6''$, and for three of these, ground based observations showed that the companion point sources are foreground galactic stars.

It has been possible for some of us to independently carry out, at the ST-ECF facility (c/o ESO, Garching bei München, Germany), a systematic visual inspection of a sample of PC frames obtained within the *HST* snapshot survey for 267 quasars (see Table 3), part of these being in the Maoz *et al.* (1992b) sample. From these observations, we have identified four HLQs whose direct image does show some structure (possibly multiple images—cf. Q1208 +1011 described in Magain *et al.* 1992a, b; cases with a superimposed galaxy image, etc.); the known quasar-foreground galactic star associations have of course been eliminated from these. Imposing also here the constraints $\theta_{DQ} \leqslant 3''$ and $MQ \leqslant 3$ mag (because the dynamical range achieved in the *HST* snapshot sample is less than that ($MQ \leqslant 5$ mag) characterizing the ground-based observations, see Sec. 2.5), we still have four GL candidates for which $OQ=1$. We estimate that approximately half of

TABLE 1. Summary of the observational characteristics of the four selected HLQ samples.

Sample	ESO-KP	Crampton et al.	Yee et al.	HST	Merged sample
N° of HLQs	187	101	104	267	469
$< z >$	2.3	2.4	2.2	2.2	2.2
$< V >$	17.5	18.1	17.7	17.6	17.7
$< M_V >$	-28.0	-27.5	-27.8	-27.8	-27.7
$< FWHM >$	1.05"	0.67"	0.76"		
N° of HLQs with					
(α)	3	0	1	0	3
(β)	21	9	2	4	31
(γ)	17	4	1		23
(δ)				4	
Most probable N° of HLQs with OQ = 1	10	2	1	2	13

(α) PQ=1
(β) OQ=1
(γ) OQ=1, $\theta_{DQ} \leq 3$" and MQ $\leq$ 5 mag.
(δ) OQ=1, $\theta_{DQ} \leq 3$" and MQ $\leq$ 3 mag.

these interesting HLQs (i.e., $\simeq$2) constitute new possible GL candidates. Let us note that we did not identify in this sample any new, yet confirmed, gravitational lens (i.e., for which $PQ=1$).

2.5 Merging the Four HLQ Samples

The most important observational characteristics of the four HLQ samples described above are listed in Table 3 (totaling 659 observations; see Surdej *et al.* 1993, Crampton *et al.* 1992, Yee *et al.* 1993, Bahcall *et al.* 1992a, and

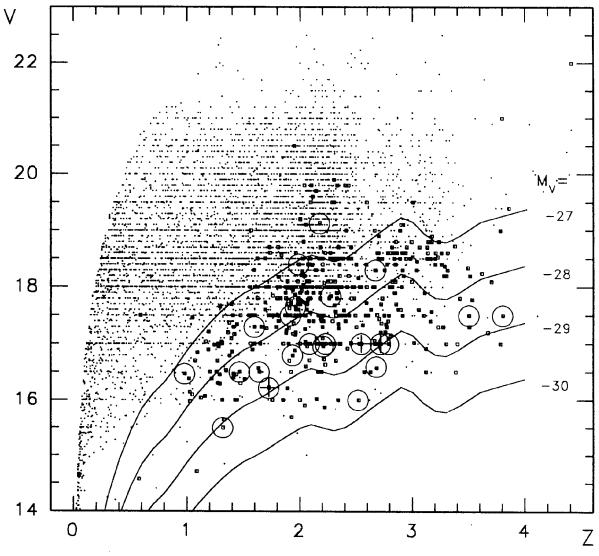

FIG. 1. Apparent magnitude (V) vs redshift (z) diagram showing the locations of 6003 quasars (very small dots) extracted from the Véron-Cetty & Véron (1991) catalogue. Note that not all apparent magnitudes quoted for the quasars in the above catalogue are visual and that most of them are just estimates. The 469 selected HLQs are shown by small squares, the 23 (although only about half of these probably consist of) possible lens candidates ($OQ=1$) by circles, and the three known lensed quasars ($PQ=1$) identified in the merged sample by crosses. Several lines of constant absolute visual magnitude are also shown.

TABLE 2. Adopted "angle selection functions" (ASFs).

1. ESO-KP sample:

1.a (type = 1, visual examination)

No solution	if θ < 0.45 FWHM
Δm = -7.5 + 16.667 θ / FWHM	if 0.45 FWHM < θ < 0.75 FWHM
Δm = 5.	if θ > 0.75 FWHM

Average seeing = 0.90"

1.b (type = 2, point spread function -PSF- subtraction)

No solution	if θ < 0.20 FWHM
Δm = -1.818 + 9.091 θ/ FWHM	if 0.20 FWHM < θ < 0.75 FWHM
Δm = 5.	if θ > 0.75 FWHM

Average seeing = 1.06"

2. Crampton et al. (type = 3):

No solution	if θ < 0.254 FWHM
Δm = -1.481 + 5.833 θ / FWHM	if 0.254 FWHM < θ < 1.111 FWHM
Δm = 5.	if θ > 1.111 FWHM

Average seeing = 0.63"

3. Yee et al. sample:

3.a (type = 4, visual examination)

No solution	if θ < 0.541 FWHM
Δm = -3.509 + 6.481 θ / FWHM	if 0.541 FWHM < θ < 1.313 FWHM
Δm = 5.	if θ > 1.313 FWHM

Average seeing = 0.70"

3.b (type = 5, comparison with contour plots of nearby stars)

No solution	if θ < 0.366 FWHM
Δm = -2.574 + 7.037 θ / FWHM	if 0.366 FWHM < θ < 1.076 FWHM
Δm = 5.	if θ > 1.076 FWHM

Average seeing = 0.76"

4. HST (type = 6, visual examination):

No solution	if θ < 0.12"
Δm = 0.300 + 5.833 θ	if 0.12" < θ < 0.46"
Δm = 3.	if θ > 0.46"

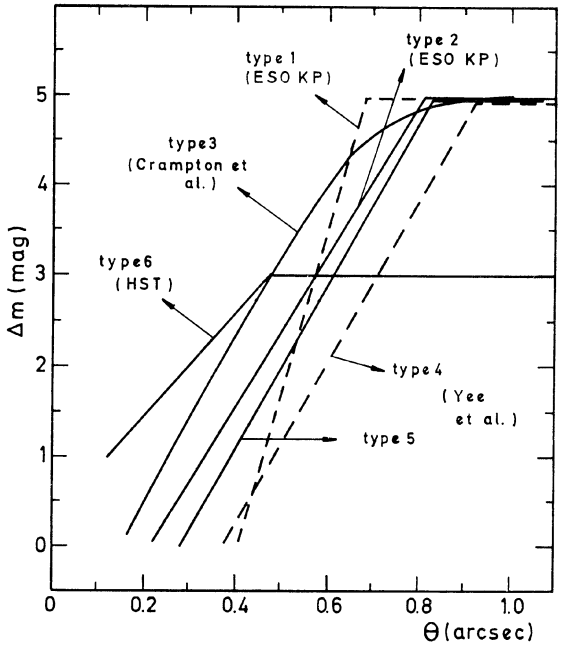

FIG. 2. The "angle selection functions" (ASFs), derived under average seeing conditions (see $\langle$FWHM$\rangle$ in Table 1), for the various types of ground based (Type=1–5, see Table 2) and *HST* (Type=6) observations. The maximum detectable magnitude difference Δm between two images is plotted here as a function of their separation θ. Whereas the *HST* angle selection function is somewhat better for $\theta \leqslant 0.4$" (equivalent to ground based seeing conditions near 0.7"), the better dynamical range of ground based CCDs accounts for better ASFs when $\theta \geqslant 0.4$".

Maoz *et al.* 1992b for more details). A summary of the observational characteristics of each sample is given in Table 1 and is also partly illustrated in Fig. 1.

Defining the "angle selection function" (ASF) as being the maximum detectable magnitude difference Δm between two pointlike images separated by an angle θ, we have listed in Table 2 these ASFs for each of the four HLQ samples and the various methods of image analysis that have been used: i.e., "Type" =1 (ESO–KP, visual examination), 2 (ESO–KP, PSF subtraction), 3 (Crampton *et al.*), 4 (Yee *et al.*, visual examination), 5 (Yee *et al.*, comparison with contour plots of nearby stars), 6 (*HST*, visual examination); see also Fig. 2.

Statistical estimates of the optical depth for gravitational macrolensing based upon the data merged from these four individual HLQ samples are reported in the next section. Note that because of observational duplication, there remains a total of 469 distinct quasars (those observations which turned out to be the best ones for the calculation of the effectiveness parameter F in Sec. 3 are indicated with an * in Table 3). In this merged sample of HLQs, we finally adopt $3 \leqslant N_L \leqslant 13$ for the observed number N_L of lenses. The lower limit corresponds to the "pessimistic" number of lenses present in the merged sample, and the upper limit to the "optimistic" number.

3. GRAVITATIONAL LENSING STATISTICS:

3.1 The Effectiveness Parameter F of Galaxy Lenses

3.1.1 The method

Following Turner *et al.* (1984, hereafter TOG) and, more recently, Nemiroff (1989), Fukugita & Turner (1991, hereafter FT), Kochanek (1991a), Mao (1991), and Schneider (1991), the effective optical depth τ of galaxies (modeled by singular isothermal spheres) to produce multiple macrolensed images of distant quasars may be expressed as

$$\tau = N_L/N_Q = F \sum_{q=1}^{N_Q} f(z_q)\, B(b_q,\Delta_{\min}) P(>\theta_q) \times \left[\frac{10^{\Delta m/2.5}-1}{10^{\Delta m/2.5}+1}\right]^2 S_{\rm cat}/N_Q, \quad (1)$$

where

—N_L represents the number of multiply imaged objects expected within a sample of N_Q quasars with redshifts z_q, blue apparent magnitudes b_q, and having been imaged under an equivalent (atmospheric or instrumental) angular resolution θ_q. Note that for all the HLQs listed in Table 3, we have derived their b_q magnitudes from their V magnitudes tabulated in the Véron-Cetty & Véron catalogue (1991) by applying an average $B-V$ correction as a function of their redshift z_q. Once more, we stress here that not all apparent magnitudes quoted for the quasars in the above catalogue are "visual" and that most of these values just constitute rough estimates.

—$F \propto n_0 \sigma^4$ measures the effectiveness of cosmically distributed "singular isothermal spherical" (SIS) galaxies to produce double QSO images (n_0 being the local number density and σ the one-component velocity dispersion of those galaxies, see TOG). From observed parameters of local galaxies and adopting an SIS model, FT, Kochanek (1991b) and Mao (1991) have calculated that $F \simeq 0.047 \pm 0.011$, with 90% contributed by E and S0 galaxies. All these authors also report that $0.023 \leqslant F \leqslant 0.047$ when the effects of a finite core radius are taken into account. Note that these estimates are independent of the value adopted for H_0 and that FT actually confirm that the core radii of E and S0 galaxies seem to be very small;

—$f(z_Q)$ accounts for the redshift dependence of the optical depth, i.e., following TOG:

$$f(z_q) = \frac{[(y^4+4y^2+1)\ln(y) - 3/2(y^4-1)]}{4(y^2-1)^2}$$

for $\Omega_0 = 0$, (empty Universe) (2)

and

$$f(z_q) = \frac{4(y^{1/2}-1)^3}{15y^{3/2}} \quad \text{for} \quad \Omega_0 = 1 \ \text{(Einstein–de Sitter)}, \quad (3)$$

where $y = (1+z_q)$,

—$B(b_q,\Delta_{\min})$ corrects for the amplification—or more appropriately, for the magnification—bias (cf. Sec. 1). For a given redshift, the magnification bias results in the observed counts of quasars being given by the convolution of the intrinsic luminosity function with a magnification probability distribution. Adopting the quasar counts $n_Q(b_q)$ reported by Hartwick & Schade (1990) and the generalized point source amplification probability $P(\Delta,\Delta_{\min})$ derived from the SIS lens model

$$P(\Delta,\Delta_{\min}) = 1.842\ 10^{0.8(\Delta_{\min}-\Delta)}, \quad (4)$$

which is such that $\int_{\Delta_{\min}}^{\infty} P(\Delta,\Delta_{\min}) d\Delta = 1$, it is straightforward to derive the following expression for the magnification bias

$$B(b_q,\Delta_{\min}) = \frac{\int_{\Delta_{\min}}^{\infty} n_Q(b_q+\Delta) P(\Delta,\Delta_{\min}) d\Delta}{n_Q(b_q)}, \quad (5)$$

for the particular value of the minimum magnitude amplification $\Delta_{\min}$. Let us note that if we were able to resolve two lensed images characterized by an infinite brightness ratio, we would have $\Delta_{\min} = 2.5 \log(2)$ (see TOG). However, because of the finite dynamical range of current imaging instruments, we have $\Delta_{\min} > 2.5 \log(2)$.

—the correction function $P(>\theta_q)$ represents the fraction of expected lenses with multiple image separations greater than the angular resolution θ_q used for observing the particular quasar(s). On the basis of numerical simulations and considering observations carried out from the ground, under optimal seeing conditions, FT have estimated that, typically, $P(>\theta_q) \simeq 50\%$–90%. Note that the function $P(>\theta_q)$ derived by FT does not depend on H_0, nor on z_q,

—the factor appearing between the brackets in Eq. (1) accounts for our inability to detect two lensed quasar im-

ages whose magnitude difference is greater than Δm. Physically, it merely accounts for the reduction in number of potential SIS lenses located along our line of sight that are capable of producing detectable multiply lensed images. Of course, the larger the instrumental dynamical range Δm, the better it is for searching for new lenses,

—finally, because of criteria imposed on the image morphology, color, proper motion, etc. while selecting quasar candidates, existing quasar catalogues are thought to be biased against the inclusion of gravitationally lensed objects. Indeed, quasar candidates might have been excluded from quasar catalogues because they appear either not to be stellarlike (e.g., made of multiple images), or somewhat redder than expected (because of a possible contamination by a deflecting galaxy) or even, possibly affected by an apparent proper motion (induced by light variability of one or more of its components). Taking into account the two first observational biases, Kochanek (1991b) has estimated that a loss of up to 30% of GL systems may result. Therefore, in order to correct for these biases, we have set $S_{\rm cat}\simeq 0.7$ in Eq. (1).

When deriving the above expression for the effective optical depth τ, TOG and FT have explicitly assumed that our ability to resolve two pointlike images in the angular range $[\theta_{\rm res}, \theta_{\rm max}]$ is characterized by a constant dynamical range Δm. This assumption naturally accounts for the presence of the factor $P(>\theta_q)\ [(10^{\Delta m/2.5}-1)/(10^{\Delta m/2.5}+1)]^2$ in Eq. (1). In our particular case, we know that the dynamical range Δm is actually a function of the angular separation θ [i.e., $\Delta m=\Delta m(\theta)$; see Table 2 and Fig. 2]. We thus have to correct Eq. (1) for this dependence and write

$$\tau=N_L/N_Q=F\sum_{q=1}^{N_Q} f(z_q)H(b_q,\text{Type},\theta_{\rm max})S_{\rm cat}/N_Q\,, \tag{6}$$

where the function

$$H(b_q,\text{Type},\theta_{\rm max}) = \frac{\int_0^{\theta_{\rm max}} p(\theta)\,B(b_q,\Delta_{\rm min}(\theta))\left[\dfrac{10^{\Delta m(\theta)/2.5}-1}{10^{\Delta m(\theta)/2.5}+1}\right]^2 d\theta}{\int_0^{\infty} p(\theta)\,d\theta} \tag{7}$$

depends of course on the particular set of observations considered (via the expression of the ASFs given in Table 2 for the different values of Type=1–6) and on the maximum angular radius $\theta_{\rm max}$ (set here to 3″) of the field under consideration. The quantity $p(\theta)d\theta$ represents the probability for the angular separation between two source images produced by an SIS lens model to lie in the range $[\theta,\theta+d\theta]$ (see the form of the function $p(\theta)$ given by FT). Furthermore, because of the limited instrumental dynamical range $\Delta m(\theta)$ that is available to resolve multiply lensed images, the argument $\Delta_{\rm min}(\theta)$ appearing in the above expression of the magnification bias must also be changed and, for the particular SIS lens model, be set equal to

$$\Delta_{\rm min}(\theta)=2.5\log\left[\frac{2(10^{\Delta m(\theta)/2.5}+1)}{(10^{\Delta m(\theta)/2.5}-1)}\right]. \tag{8}$$

3.1.2 Numerical applications and results

We consider together the ESO–KP, Crampton *et al.*, Yee *et al.*, and *HST* snapshot samples of 469=(187 U 101 U 104 U 267) HLQs (see Table 3), for which we have also listed in Table 1 the numbers N_L^O (optimistic estimate) and N_L^P (pessimistic estimate) of possible lens candidates and known cases of gravitational lensing, respectively. We have then derived by means of Eq. (6) lower and upper limits for the effectiveness parameter F, taking into account the dependence of the functions $f(z_q)$ and $H(B_q,\text{Type},\theta_{\rm max})$ for each HLQ, assuming various types of cosmologies (cf. different values of the normalized cosmological parameter $\lambda_0=\Lambda/3H_0^2$). Conversely, we have adopted the range of values $0.023<F<0.047$, inferred by FT for the effectiveness parameter F of SIS galaxies, and we have derived upper ($N_{\rm up}^{\rm exp}$) and lower ($N_{\rm lo}^{\rm exp}$) estimates for the expected numbers of lenses. Our results are summarized in Table 4.

3.1.3 Discussion

For the case of an Einstein–de Sitter cosmology ($\Omega_0=1$, $\Lambda=0$), we find that, at a 99.7% confidence level, $0.005<F<0.478$. This large interval of values encompasses the predicted value $F=0.047\pm0.011$ for the case of a singular isothermal sphere and $0.023\leqslant F\leqslant 0.047$ when the effects of a finite core radius are taken into account (see FT, Kochanek 1991b, and Mao 1991). Furthermore, our statistical results seem to confirm the claims by Turner (1990), Fukugita *et al.* (1990, hereafter FFK), Fukugita *et al.* (1992, hereafter FFKT), FT and others that flat universe models excessively dominated by the cosmological constant are not favored. However, due to a number of complications discussed hereafter, the possibility of estimating the cosmological parameter Λ from the observed rate of quasars being lensed by galaxies should be considered presently with great caution.

Indeed, whereas the optical depth τ is quite sensitive to the cosmological parameter Λ (cf. Turner 1990, FFK, Mao 1991, FFKT, FT, Kochanek 1991c), it also depends very strongly on various other factors. For instance:

(i) τ depends on Ω_0 as well as on the assumed (large) degree of homogeneity of the Universe;

(ii) τ depends on the adopted distribution of galaxy types, on the exact form of the velocity dispersion, which is itself closely related to the (Schechter) luminosity function as well as on the accuracy and applicability of the observed luminosity—velocity dispersion (Faber–Jackson) or rotation curve (Tully–Fischer) relations. It also depends on the implicit existence of massive dark halos around elliptical galaxies (for which $\sigma_{\rm eff}=\sigma\sqrt{3/2}$ and on the adopted mass distribution ($\rho\propto 1/r^2$) for elliptical, spiral, etc. galaxies;

(iii) following Kochanek (1991b), the optical depth τ could also be quite sensitive to reddening effects induced by the lensing galaxies, if they are significant at all;

TABLE 3. Observational characteristics of the HLQs (see notes below).

Identification		F	Type	z	m	M	FWHM	PQ	OQ	θ_{DQ}	MQ
Q	0002-422	*	1	2.758	17.21	-28.8	0.65	0	0		
UM	197		4	2.180	18.70	-26.7	0.78	0	0		
UM	197		1	2.180	18.00	-27.4	1.15	0	0		
UM	197		6	2.180	18.00	-27.4		0	0		
UM	197	*	3	2.180	18.00	-27.4	0.90	0	0		
UM	18	*	1	1.890	16.21	-29.1	0.70	0	0		
UM	18		5	1.890	16.21	-29.1	0.86	0	0		
UM	18		6	1.890	16.21	-29.1		0	0		
TEX	0004+171	*	6	2.890	18.50	-27.7		0	0		
PKS	0005-239	*	1	1.410	16.47	-28.2	0.67	0	0		
Q	0007-4239	*	1	2.670	18.30	-27.6	0.94	0	1	2.4	4.5
Q	0007-354	*	6	2.030	18.04	-27.4		0	0		
UM	208		4	2.310	18.50	-27.2	0.66	0	0		
UM	208		1	2.310	17.00	-28.7	0.72	0	0		
UM	208		6	2.310	17.00	-28.7		0	0		
UM	208	*	3	2.310	17.00	-28.7	0.57	0	0		
UM	209	*	1	1.560	17.00	-27.9	0.53	0	0		
PKS	0008+171	*	4	1.601	18.00	-26.9	0.75	0	0		
UM	211	*	3	2.000	16.00	-29.4	0.63	0	0		
Q	0011-012	*	1	2.230	17.00	-28.4	1.00	0	1	3.0	2.0
UM	224	*	1	2.086	17.00	-28.5	0.62	0	1	0.0	0.0
UM	224		6	2.086	17.00	-28.5		0	0		
UM	224		4	2.086	18.20	-27.3	0.66	0	1	3.3	5.4
UM	224		3	2.090	17.00	-28.5	0.65	0	1	3.2	5.6
S5	0014+81		6	3.384	16.50	-29.3		0	0		
S5	0014+81	*	3	3.384	16.50	-29.3	0.70	0	0		
3C	9.0	*	5	2.012	18.21	-27.2	0.66	0	0		
Q	0018-422		1	2.860	18.60	-27.6	1.12	0	0		
Q	0018-422	*	6	2.860	18.60	-27.6		0	0		
UM	663	*	6	2.000	17.90	-27.5		0	0		
UM	30		6	2.050	19.10	-26.3		0	0		
UM	30	*	3	2.050	18.00	-27.4	0.55	0	0		
UM	35		5	2.420	18.00	-27.8	0.66	0	0		
UM	35	*	3	2.420	18.00	-27.8	0.68	0	0		
UM	247	*	3	2.350	17.00	-28.7	0.60	0	0		
UM	42	*	3	2.260	18.00	-27.4	0.67	0	0		
UM	252	*	4	1.732	18.60	-26.5	0.68	0	0		
UM	253	*	2	2.222	18.60	-26.8	0.72	0	0		
UM	253		4	2.222	18.60	-26.8	0.70	0	0		
UM	665		6	2.650	18.00	-27.8		0	0		
UM	665	*	4	2.650	18.00	-27.8	0.70	0	0		
	0029+0722	*	5	3.259	18.40	-27.3	0.58	0	0		
	0029+0722		6	3.259	18.40	-27.3		0	0		
	0029+0722		3	3.272	18.40	-27.3	0.75	0	0		
UM	45	*	1	1.990	18.40	-27.0	0.71	0	1	0.0	0.0
UM	46	*	3	2.310	18.00	-27.7	0.46	0	0		
UM	259	*	1	1.850	17.00	-28.2	0.77	0	0		
UM	259		4	1.850	17.00	-28.2	0.69	0	0		
4C	09.01	*	1	1.918	17.50	-27.8	0.89	0	1	0.0	0.0
4C	09.01		6	1.918	17.50	-27.8		0	0		
4C	09.01		4	1.918	17.50	-27.8	1.22	0	0		
Q	0034-3308	*	1	2.180	17.80	-27.6	1.06	0	0		
UM	52	*	4	2.270	18.00	-27.4	0.67	0	0		
5C	03.44	*	6	1.937	17.95	-27.4		0	0		
Q	0038-3936	*	6	2.370	18.00	-27.8		0	0		
CT	15	*	1	1.803	17.50	-27.7	0.75	0	0		
Q	0039-265	*	6	1.803	17.50	-27.7		0	0		
	0041-2707	*	1	2.783	17.40	-28.6	0.69	0	0		
Q	0041-261	*	1	2.501	17.30	-28.3	0.96	0	0		
	0042-2627	*	1	3.400	17.00	-28.8	0.74	0	0		
UM	275	*	1	2.150	17.00	-28.4	0.64	0	0		
UM	275		6	2.150	17.00	-28.4		0	0		
UM	275		4	2.150	17.00	-28.4	1.34	0	0		
UM	275		3	2.150	17.00	-28.4	0.66	0	0		
UM	276	*	6	1.590	18.30	-26.6		0	0		
UM	667		6	3.135	18.60	-27.2		0	0		
UM	667	*	3	3.140	18.60	-27.2	0.88	0	0		
UM	278		6	2.530	18.00	-27.6		0	0		
UM	278	*	4	2.530	18.00	-27.6	0.52	0	0		
UM	278		3	2.530	18.00	-27.6	0.76	0	0		
PKS	0046-06	*	5	2.060	18.00	-27.5	0.52	0	0		
PKS	0046-315	*	6	2.721	17.70	-28.2		0	0		
UM	281	*	1	1.870	17.90	-27.4	0.66	0	0		
UM	281		6	1.870	17.90	-27.4		0	0		
Q	0048-261	*	6	2.249	18.10	-27.3		0	0		
CS	73	*	6	2.272	18.10	-27.3		0	0		
UM	287	*	1	2.270	17.00	-28.4	0.72	0	0		
UM	287		6	2.270	17.00	-28.4		0	0		
UM	287		4	2.270	17.00	-28.4	0.73	0	0		
Q	0049-393	*	6	2.845	17.90	-28.2		0	0		
UM	288	*	1	2.310	17.00	-28.7	0.68	0	0		
UM	288		5	2.310	17.00	-28.7	0.68	0	0		
UM	288		6	2.310	17.00	-28.7		0	0		
UM	288		3	2.310	17.00	-28.7	0.75	0	0		
B2	0051+29	*	6	1.828	17.80	-27.4		0	0		
Q	0052-4104	*	6	2.060	18.10	-27.4		0	0		
DH	0054-284	*	1	3.614	18.24	-27.8	1.50	0	0		
PKS	0054-006	*	4	2.795	18.00	-28.1	0.52	0	0		
PKS	0054-006		3	2.795	18.00	-28.1	0.74	0	0		
Q	0055-3844	*	6	2.350	18.40	-27.3		0	0		
	0055-2659	*	1	3.670	17.20	-28.9	0.76	0	0		
UM	294	*	4	1.920	17.70	-27.6	0.67	0	0		
Q	0056-3924	*	6	1.409	17.30	-27.4		0	0		
	0057-358	*	1	1.550	17.50	-27.4	0.57	0	0		
PHL	938	*	5	1.959	17.16	-28.2	0.59	0	0		
	0059-370	*	1	2.210	17.50	-27.9	0.56	0	0		
Q	0059-4110	*	6	1.960	18.00	-27.4		0	0		
Q	0059-2735	*	1	1.595	17.00	-27.9	0.70	0	0		
PKS	0100-270	*	6	1.597	17.50	-27.4		0	0		
PHL	957	*	5	2.681	16.57	-29.3	0.54	0	0		
PHL	957		3	2.681	16.60	-29.3	0.60	0	1	0.0	0.0
Q	0100-3955	*	6	2.500	18.40	-27.2		0	0		
Q	0101-4216	*	6	1.900	17.50	-27.8		0	0		
	0101-353	*	1	2.200	17.30	-28.1	0.52	0	0		
Q	0102-4238	*	1	2.330	18.00	-27.5	1.70	0	0		
UM	669	*	6	3.035	18.30	-27.7		0	0		
Q	0103-29	*	6	2.800	18.60	-27.5		0	0		
Q	0105-391	*	6	2.310	18.10	-27.5		0	0		
UM	86	*	4	1.960	17.20	-28.2	0.68	0	0		
	0105-2634	*	2	3.505	17.30	-28.6	0.70	0	0		
PKS	0106+01	*	4	2.107	18.39	-27.1	0.68	0	0		
PKS	0109+17		6	2.157	18.00	-27.4		0	0		
PKS	0109+17		4	2.157	18.00	-27.4	0.63	0	0		
PKS	0109+17	*	3	2.157	18.00	-27.4	0.43	0	0		
Q	0109-353	*	6	2.406	17.40	-28.3		0	0		
	0112-329	*	6	1.588	17.50	-27.4		0	0		
UM	670	*	5	3.160	17.40	-28.4	0.55	0	0		
UM	670		6	3.160	17.40	-28.4		0	0		
	0115-376	*	1	1.810	17.50	-27.7	0.84	0	0		
UM	314	*	3	2.190	17.00	-28.4	0.59	0	0		
UM	315		6	2.050	18.00	-27.4		0	0		
UM	315	*	3	2.050	18.00	-27.4	0.73	0	0		
UM	671	*	6	1.790	17.30	-27.9		0	0		
	0119-358	*	6	1.797	17.80	-27.4		0	0		
B2	0119+24	*	4	2.025	18.50	-26.9	0.55	0	0		
PKS	0119-04		1	1.955	16.88	-28.5	1.00	0	0		
PKS	0119-04	*	5	1.955	16.88	-28.5	0.68	0	0		
PKS	0119-04		6	1.955	16.88	-28.5		0	0		
	0121-329	*	1	2.325	17.90	-27.8	0.78	0	0		
	0121-329		6	2.325	17.90	-27.8		0	0		
Q	0122-380	*	1	2.190	16.50	-28.9	0.83	0	0		
Q	0122-380		6	2.190	16.50	-28.9		0	0		
PKS	0122-00	*	6	1.070	16.70	-27.3		0	0		
	0123-527	*	1	2.320	16.70	-29.0	1.38	0	0		
Q	0123-365	*	6	2.457	18.50	-27.0		0	0		
PKS	0123+25	*	4	2.358	17.50	-27.9	0.53	0	0		
PKS	0123+25		3	2.358	17.50	-27.9	0.88	0	0		
	0124-323	*	1	2.200	17.50	-27.9	0.84	0	0		
UM	327	*	3	2.070	18.00	-27.5	0.82	0	0		
Q	0125-400	*	1	1.390	17.10	-27.6	0.76	0	0		
Q	0125-400		6	1.390	17.10	-27.6		0	0		
UM	104	*	6	1.620	17.80	-27.2		0	0		
	0126-349	*	2	2.080	18.00	-27.5	1.29	0	0		
	0127-557	*	1	2.210	17.40	-28.0	0.75	0	0		
	0128-525	*	1	2.380	17.50	-28.1	0.70	0	0		
Q	0130-403	*	1	3.015	17.02	-29.0	0.67	0	0		
Q	0130-403		6	3.015	17.02	-29.0		0	0		
	0131+0120	*	3	3.793	21.00	-25.2	0.63	0	0		
NAB	0132+20	*	5	1.782	17.50	-27.7	0 48	0	0		
NAB	0132+20		6	1.782	17.50	-27.7		0	0		
UM	672	*	6	3.130	18.70	-27.1		0	0		
UM	349	*	6	2.150	18.00	-27.4		0	0		
PKS	0136-231	*	6	1.893	18.00	-27.3		0	0		
PKS	0136+176	*	6	2.730	18.50	-27.5		0	0		
UM	356		6	2.240	18.00	-27.4		0	0		
UM	356	*	3	2.240	18.00	-27.4	0.63	0	0		
Q	0138-381	*	6	2.874	17.60	-28.6		0	0		
Q	0140-306	*	6	3.130	18.50	-27.3		0	0		
UM	673	*	2	2.719	17.00	-28.9	0.95	1	1	2.2	2.2
UM	366	*	6	3.138	18.80	-27.0		0	0		
UM	368		6	3.160	18.50	-27.3		0	0		
UM	368	*	3	3.160	18.50	-27.3	0.70	0	0		
TEX	0145+386	*	6	1.440	16.00	-28.7		0	0		
UM	139		6	2.030	18.80	-26.6		0	0		
UM	139	*	3	2.030	18.00	-27.4	0.88	0	0		
UM	141	*	1	2.909	18.60	-27.6	0.60	0	0		
UM	141		3	2.909	17.00	-29.2	0.89	0	0		
UM	142	*	6	1.390	17.70	-27.0		0	0		
UM	674	*	3	2.840	18.60	-27.5	1.00	0	0		
Q	0149-397	*	6	2.058	17.90	-27.6		0	0		
UM	675	*	6	2.147	17.10	-28.4		0	0		
UM	375		6	2.020	18.00	-27.4		0	0		

TABLE 3. (continued)

Identification		F	Type	z	m	M	FWHM	PQ	OQ	θ_{DQ}	MQ
UM	375	*	3	2.020	18.00	-27.4	0.66	0	0		
PHL	1222		6	1.904	17.63	-27.7		0	0		
PHL	1222	*	4	1.904	17.63	-27.7	0.65	0	0		
S5	0153+74		6	2.338	16.00	-29.8		0	0		
S5	0153+74	*	3	2.338	16.00	-29.8	0.88	0	0		
UM	148	*	1	2.991	18.80	-27.3	0.62	0	0		
	0154-512U	*	6	1.660	17.30	-27.7		0	0		
UM	154	*	5	2.432	18.20	-27.7	0.63	0	0		
B2	0201+36B	*	6	2.912	17.50	-28.7		0	0		
	0203-498	*	2	2.540	18.00	-27.7	1.42	0	0		
Q	0205-379	*	6	2.404	17.40	-28.1		0	0		
UM	400	*	6	1.890	18.10	-27.2		0	0		
UM	402		1	2.856	17.70	-28.4	1.07	0	0		
UM	402		4	2.856	17.70	-28.4	0.69	0	0		
UM	402	*	3	2.840	16.00	-30.1	0.55	0	0		
UM	403		1	2.190	18.00	-27.4	1.57	0	0		
UM	403		4	2.190	18.00	-27.4	0.65	0	0		
UM	403	*	3	2.190	18.00	-27.4	0.89	0	0		
Q	0207-398	*	2	2.805	17.15	-28.9	1.21	0	0		
Q	0207-398		6	2.805	17.15	-28.9		0	0		
TEX	0215+165	*	6	1.900	18.00	-27.3		0	0		
	0216+0803		6	2.993	18.10	-28.0		0	0		
	0216+0803		4	2.993	18.10	-28.0	0.72	0	0		
	0216+0803	*	3	2.991	18.10	-28.0	0.53	0	0		
Q	0222-415		1	2.000	17.70	-27.7	1.34	0	0		
Q	0222-415	*	6	2.000	17.70	-27.7		0	0		
PKS	0225-014	*	3	2.037	18.20	-27.2	0.48	0	0		
PKS	0226-038	*	5	2.064	16.96	-28.5	0.70	0	0		
PKS	0226-038		6	2.064	16.96	-28.5		0	0		
PKS	0229+13		6	2.065	17.71	-27.8		0	0		
PKS	0229+13		4	2.065	17.71	-27.8	0.64	0	0		
PKS	0229+13	*	3	2.065	17.70	-27.8	0.67	0	0		
PKS	0232-04	*	1	1.434	16.46	-28.3	0.75	0	0		
PKS	0232-01		6	1.434	16.46	-28.3		0	0		
PKS	0234-301	*	2	2.102	18.00	-27.5	1.16	0	0		
PKS	0237-23	*	1	2.224	16.63	-28.8	0.71	0	0		
UM	677		1	2.782	18.60	-27.4	1.74	0	0		
UM	677	*	6	2.782	18.60	-27.4		0	0		
PKS	0244-128	*	1	2.201	17.10	-28.3	0.58	0	0		
PKS	0244-128		6	2.201	17.10	-28.3		0	0		
PKS	0244-128		4	2.201	17.10	-28.3	0.70	0	0		
S4	0248+43	*	6	1.316	15.50	-29.0		0	1	0.6	2.5
UM	678		2	3.202	18.40	-27.3	1.66	0	0		
UM	678	*	6	3.202	18.40	-27.3		0	0		
UM	679		2	3.205	18.60	-27.1	1.66	0	0		
UM	679	*	6	3.205	18.60	-27.1		0	0		
Q	0254-404	*	2	2.290	17.40	-27.6	1.19	0	0		
Q	0254-404		6	2.280	17.40	-27.9		0	0		
Q	0254-334	*	1	1.849	16.00	-29.2	0.66	0	0		
Q	0256-0000	*	5	3.374	18.72	-27.1	0.64	0	0		
Q	0256-0000		3	3.367	18.70	-27.1	0.75	0	0		
Q	0301-0035		2	3.223	18.53	-27.2	1.30	0	0		
Q	0301-0035		6	3.223	18.53	-27.2		0	0		
Q	0301-0035	*	3	3.205	18.50	-27.2	0.67	0	0		
Q	0302-0019		1	3.286	18.37	-27.4	1.17	0	0		
Q	0302-0019		6	3.286	18.37	-27.4		0	0		
Q	0302-0019	*	3	3.285	18.40	-27.3	0.60	0	0		
	0302+1705	*	3	2.890	19.00	-27.2	0.61	0	0		
EX	0302-223	*	1	1.409	16.40	-28.3	0.63	0	0		
EX	0302-223		6	1.409	16.40	-28.3		0	0		
Q	0304-392		1	1.965	17.60	-27.8	1.14	0	0		
Q	0304-392	*	6	1.965	17.60	-27.8		0	0		
UM	682		1	2.752	18.30	-27.7	1.23	0	0		
UM	682	*	6	2.752	18.30	-27.7		0	0		
	0308+1902	*	3	2.835	18.60	-27.5	0.52	0	0		
PKS	0317-02	*	3	2.092	19.50	-26.0	0.65	0	0		
Q	0321-337	*	1	1.985	17.81	-27.6	1.18	0	0		
Q	0324-407	*	6	3.056	17.60	-28.4		0	0		
PKS	0329-255	*	1	2.685	17.51	-28.4	0.80	0	0		
PKS	0329-255		6	2.685	17.51	-28.4		0	0		
Q	0329-385	*	6	2.423	16.92	-28.7		0	0		
H	0333-380	*	1	2.201	18.50	-26.9	1.13	0	0		
H	0335-336	*	1	2.265	18.50	-26.9	1.12	0	0		
Q	0338-394	*	6	2.590	18.40	-27.3		0	0		
PKS	0347-241	*	1	1.885	17.50	-27.8	1.24	0	0		
Q	0347-383	*	1	3.230	17.30	-28.4	0.84	0	0		
Q	0347-383		6	3.230	17.30	-28.4		0	0		
NAB	0348+06		5	2.060	17.60	-27.9	0.87	0	0		
NAB	0348+06		6	2.060	17.60	-27.9		0	0		
NAB	0348+06	*	3	2.058	17.60	-27.9	0.62	0	0		
UM	684	*	6	2.819	18.00	-28.1		0	0		
Q	0353-383		1	1.959	17.50	-27.9	1.57	0	0		
Q	0353-383	*	6	1.959	17.50	-27.9		0	0		
PKS	0355-483	*	6	1.016	16.38	-27.5		0	0		
DW	0400+258	*	3	2.109	18.00	-27.5	0.54	0	1	3.2	0.7
PKS	0402-362	*	6	1.417	17.17	-27.5		0	0		
PKS	0405-12	*	1	0.574	14.57	-28.1	1.27	0	0		
PKS	0406-127	*	4	1.563	19.00	-25.9	0.58	0	0		
	0420+003	*	1	2.918	19.10	-27.1	1.06	0	1	4.4	3.4
Q	0420-388	*	1	3.120	16.92	-28.9	0.88	0	0		
Q	0420-388		6	3.120	16.92	-28.9		0	0		
PKS	0421+019	*	5	2.048	17.04	-28.4	0.80	0	0		
PKS	0421+019		6	2.048	17.04	-28.4		0	0		
PKS	0424-13	*	5	2.165	17.50	-27.9	0.76	0	0		
1E	0438-166	*	2	1.960	17.65	-27.7	1.37	0	1	0.0	0.0
1E	0438-166		6	1.960	17.65	-27.7		0	0		
PKS	0438-43	*	2	2.852	18.80	-27.3	1.07	0	0		
PKS	0445+09	*	3	2.110	19.60	-25.9	0.45	0	0		
Q	0447-395	*	6	1.980	18.10	-27.3		0	0		
PKS	0448-392		1	1.288	16.46	-28.0	1.16	0	0		
PKS	0448-392	*	6	1.288	16.46	-28.0		0	0		
Q	0453-423	*	1	2.661	17.06	-28.8	0.68	0	0		
Q	0453-423		6	2.661	17.06	-28.8		0	0		
PKS	0454+039	*	2	1.345	16.53	-28.1	1.06	0	0		
PKS	0454+039		6	1.345	16.53	-28.1		0	0		
PKS	0457+024	*	3	2.384	18.50	-27.4	0.45	0	0		
PKS	0458-02	*	3	2.286	19.50	-26.3	0.61	0	1	5.3	2.5
PKS	0504+03	*	3	2.453	18.70	-26.8	0.60	0	0		
PKS	0506-61	*	6	1.093	16.85	-27.2		0	0		
PKS	0514-16	*	6	1.278	16.95	-27.5		0	0		
PKS	0528-250	*	6	2.765	17.34	-28.7		0	0		
Q	0551-366	*	2	2.317	17.57	-28.0	1.35	0	0		
Q	0551-366		6	2.317	17.57	-28.0		0	0		
B2	0552+39A	*	3	2.365	18.00	-27.7	0.51	0	1	3.3	4.9
PKS	0743-67	*	6	1.510	16.37	-28.5		0	0		
SBS	0747+611	*	6	2.492	17.50	-28.1		0	0		
B2	0749+37	*	6	1.200	16.50	-27.8		0	0		
B2	0808+28	*	6	1.910	18.00	-27.3		0	0		
B2	0812+33A		6	2.420	18.00	-27.8		0	0		
B2	0812+33A	*	4	2.420	18.00	-27.8	0.70	0	0		
PKS	0819-032	*	2	2.352	18.20	-27.6	1.27	0	0		
PKS	0819-032		6	2.352	18.20	-27.6		0	0		
B2	0820+29	*	4	2.368	18.50	-27.3	0.75	0	0		
	0822+27W1	*	6	2.060	17.70	-27.8		0	0		
B2	0827+24	*	6	2.046	17.26	-28.2		0	0		
	0830+112	*	6	0.589	17.50	-25.3		0	0		
	0831+1248	*	6	2.734	17.80	-28.2		0	0		
4C	19.31	*	5	1.691	17.73	-27.3	0.72	0	0		
S5	0836+71	*	6	2.160	16.50	-28.9		0	0		
US	1443	*	6	1.564	17.50	-27.4		0	0		
4C	13.39	*	5	1.875	17.80	-27.5	0.75	0	0		
4C	13.39		6	1.875	17.80	-27.5		0	0		
Q	0846+1540	*	2	2.912	18.30	-27.9	1.07	0	0		
Q	0846+1540		6	2.912	18.30	-27.9		0	0		
Q	0846+1540		4	2.912	18.30	-27.9	0.93	0	0		
	0847.6+156A	*	6	2.660	18.00	-27.8		0	0		
LB	8755	*	6	2.014	17.93	-27.5		0	0		
LB	8863	*	6	2.214	18.07	-27.3		0	0		
LB	8956	*	6	1.891	17.70	-27.6		0	0		
	0903+1534	*	6	2.655	18.00	-27.8		0	0		
H	0903+175	*	6	2.771	17.30	-28.7		0	0		
H	0903+175		4	2.771	17.30	-28.7	0.80	0	0		
B3	0907+381	*	6	2.160	18.00	-27.4		0	0		
	0913+0715	*	6	2.785	17.10	-28.9		0	0		
GB2	0932+367	*	6	2.840	18.50	-27.6		0	0		
Q	0932+501	*	6	1.880	17.24	-28.0		0	0		
TB	0933+733	*	6	2.528	17.00	-28.6		0	0		
B2	0941+26		6	2.906	18.00	-28.2		0	0		
B2	0941+26	*	4	2.906	18.00	-28.2	0.68	0	0		
US	987	*	6	1.892	17.99	-27.3		0	0		
PKS	0945-321	*	1	2.140	18.30	-27.2	1.18	0	0		
PG	0946+301	*	6	1.216	16.38	-28.0		0	0		
SBS	0953+549	*	6	2.584	17.50	-28.2		0	0		
PC	0955+4717	*	5	2.482	17.80	-27.8	0.77	0	0		
PC	0955+4717		6	2.482	17.80	-27.8		0	0		
	0956+1217	*	6	3.301	18.20	-27.5		0	0		
	0957-055	*	2	1.810	17.40	-27.8	1.07	0	0		
MAR	132	*	6	1.754	16.00	-29.1		0	0		
	1002-249	*	2	2.437	17.50	-28.4	1.20	0	0		
PG	1008+133	*	6	1.287	16.29	-28.2		0	0		
H	1011+091		1	2.260	17.80	-27.6	1.14	0	0		
H	1011+091	*	6	2.260	17.80	-27.6		0	0		
B2	1011+25	*	5	1.631	16.57	-28.4	0.81	0	0		
TON	34	*	5	1.924	15.69	-29.6	0.88	0	0		
PKS	1022-102	*	2	2.000	17.00	-28.4	0.75	0	0		
TO	10370-271	*	6	2.193	17.40	-28.0		0	0		
TO	10382-272	*	6	2.331	17.90	-27.7		0	0		
4C	06.41	*	6	1.270	16.70	-27.8		0	0		
S5	1039+81	*	6	1.260	16.50	-27.9		0	0		
SBS	1039+582	*	6	1.472	17.50	-27.3		0	0		
4C	60.15	*	6	1.722	17.50	-27.6		0	0		
	1055.4+022	*	2	2.730	17.80	-28.2	1.15	0	0		

TABLE 3. (continued)

Identification		F	Type	z	m	M	FWHM	PQ	OQ	θ_{DQ}	MQ
SBS	1055+584	*	6	2.239	18.00	-27.4		0	0		
Q	1101-264	*	2	2.148	16.02	-29.4	1.02	0	0		
PG	1115+080	*	2	1.724	16.22	-28.9	1.38	1	1	0.5	0.1
SBS	1116+603	*	6	2.628	16.50	-29.3		0	0		
SBS	1117+535	*	6	1.921	18.00	-27.3		0	0		
UM	425	*	2	1.465	16.50	-28.3	1.23	0	1	0.0	0.0
PKS	1123+26	*	4	2.341	18.50	-27.3	0.86	0	0		
PKS	1127-14	*	1	1.187	16.90	-27.4	0.89	0	0		
PKS	1127-14		6	1.187	16.90	-27.4		0	0		
	1136+1214	*	2	2.894	17.60	-28.6	1.37	0	0		
	1136+1214		6	2.894	17.60	-28.6		0	0		
	1136+1214		4	2.894	17.60	-28.6	0.79	0	0		
US	2778	*	6	1.578	16.90	-28.0		0	0		
SBS	1138+584	*	6	1.699	18.00	-27.1		0	0		
PG	1138+040	*	2	1.877	17.19	-28.1	1.12	0	0		
PG	1138+040		5	1.877	17.19	-28.1	0.78	0	0		
US	2813	*	6	1.691	17.60	-27.5		0	0		
PKS	1148-00		1	1.982	17.60	-27.8	1.43	0	0		
PKS	1148-00	*	6	1.982	17.60	-27.8		0	0		
B2	1148+38	*	6	1.303	17.04	-27.5		0	0		
POX	5B	*	2	2.207	17.00	-28.4	1.61	0	0		
PKS	1157+014	*	6	1.986	17.74	-27.6		0	0		
POX	42	*	1	2.453	17.01	-28.5	0.99	0	0		
Q	1159+123	*	2	3.502	17.50	-28.4	1.14	0	1	0.5	0.2
Q	1159+123		6	3.502	17.50	-28.4		0	0		
POX	61	*	6	2.455	17.80	-27.7		0	0		
PG	1206+459	*	6	1.158	16.07	-28.1		0	0		
	1206+1155	*	6	3.106	17.90	-28.0		0	0		
	12076+399	*	1	2.100	17.50	-27.8	1.17	0	0		
	1208+1011	*	2	3.803	17.50	-28.7	1.38	0	1	0.4	1.4
	1208+1011		6	3.802	17.50	-28.7		0	1	0.4	1.3
Q	1213+0922	*	1	2.719	17.20	-28.7	0.94	0	0		
Q	1213+0922		6	2.719	17.20	-28.7		0	0		
UM	485	*	1	2.690	17.00	-28.9	1.49	0	0		
B2	1215+33		5	2.606	17.50	-28.3	1.11	0	0		
B2	1215+33	*	6	2.606	17.50	-28.3		0	0		
MC	1215+113	*	6	1.396	16.86	-27.8		0	0		
SBS	1221+545	*	6	2.106	18.00	-27.5		0	0		
	1222+023	*	1	2.050	17.00	-28.4	0.99	0	0		
TON	1530	*	5	2.051	16.60	-28.8	0.87	0	0		
B2	1225+31	*	5	2.219	15.87	-29.5	1.14	0	0		
	1228.7+07.7	*	6	2.391	17.59	-28.0		0	0		
PG	1241+176	*	1	1.273	16.30	-28.2	0.95	0	1	3.1	6.5
PG	1241+176		6	1.273	16.30	-28.2		0	0		
	1244.9+34.7	*	6	2.480	18.00	-27.6		0	0		
BSO	1	*	6	1.241	16.98	-27.4		0	0		
Q	1246-057	*	1	2.212	16.73	-28.7	1.25	0	0		
PG	1247+268	*	5	2.041	15.90	-29.5	0.76	0	0		
PG	1247+268		6	2.041	15.90	-29.5		0	0		
PG	1254+047	*	6	1.024	16.14	-27.7		0	0		
B	201	*	6	1.375	16.79	-27.8		0	0		
W	61972	*	6	1.922	17.75	-27.6		0	0		
BSO	6	*	6	1.956	17.87	-27.5		0	0		
W	22722	*	6	1.759	17.85	-27.3		0	0		
W	21511	*	6	2.047	17.72	-27.7		0	0		
POX	123	*	6	2.289	18.00	-27.7		0	0		
4C	18.36	*	5	1.689	18.50	-26.6	0.89	0	0		
Q	1309-056	*	2	2.185	17.44	-28.0	1.05	0	0		
Q	1309-056		6	2.185	17.44	-28.0		0	0		
PKS	1311-270	*	1	2.195	17.43	-28.0	0.75	0	0		
PKS	1311-270		6	2.195	17.43	-28.0		0	0		
BSO	11	*	3	2.084	18.40	-27.1	0.68	0	0		
UM	557	*	1	2.687	18.60	-27.3	1.09	0	0		
SBS	1315+605	*	6	1.981	18.00	-27.4		0	0		
PC	1315+4722	*	3	2.592	18.00	-27.7	0.60	0	0		
TON	153	*	6	1.022	15.98	-27.9		0	0		
Q	1317-0507	*	1	3.700	18.10	-28.0	1.00	0	0		
Q	1318-113	*	6	2.308	17.68	-27.4		0	0		
PKS	1318+111	*	1	2.172	19.13	-26.3	1.30	0	1	1.5	3.0
TON	155		6	1.703	17.27	-27.8		0	0		
TON	155	*	5	1.703	17.27	-27.8	0.87	0	0		
POX	188	*	2	2.360	17.00	-28.8	1.00	0	0		
Q	1323-0248	*	1	2.121	17.40	-28.1	0.90	0	0		
PKS	1327-206	*	6	1.165	17.04	-27.2		0	0		
PG	1329+412	*	4	1.935	17.18	-28.2	1.10	0	0		
Q	1330+0108	*	2	3.510	18.20	-27.8	1.38	0	0		
MC	1331+170	*	2	2.084	16.71	-28.8	1.29	0	0		
MC	1331+170		5	2.084	16.71	-28.8	0.91	0	0		
UM	590	*	2	2.790	17.00	-29.0	0.88	0	1	0.2	0.5
	1337+1121	*	6	2.919	18.20	-28.0		0	0		
Q	1338-018	*	1	2.079	17.40	-28.1	1.00	0	0		
	1340+0959	*	2	2.942	18.50	-27.7	1.26	0	0		
4C	58.27	*	6	2.039	17.50	-27.9		0	0		
Q	1346-036		2	2.345	17.27	-28.5	1.94	0	0		
Q	1346-036	*	6	2.345	17.27	-28.5		0	0		
	1347+1116	*	6	2.697	18.50	-27.4		0	0		
Q	1349+001	*	2	1.426	16.00	-28.7	1.42	0	0		
PG	1352+011	*	6	1.121	16.04	-28.1		0	0		
PKS	1354+25	*	3	2.032	18.00	-27.4	0.63	0	0		
4C	58.29	*	6	1.371	17.37	-27.3		0	0		
SP	1	*	3	3.300	17.00	-28.7	0.73	0	0		
	1358+1134	*	2	2.571	16.50	-29.2	1.34	0	0		
	1358+1134		5	2.571	16.50	-29.2	0.89	0	0		
	1358+1134		6	2.571	16.50	-29.2		0	0		
	1400+1126	*	6	3.174	18.90	-26.9		0	0		
	1400+0935	*	6	2.980	18.50	-27.6		0	0		
PKS	1402-012	*	6	2.519	18.16	-27.5		0	0		
PKS	1402-012		1	2.519	18.16	-27.5	1.30	0	0		
PKS	1402+044	*	6	3.202	18.50	-27.2		0	0		
PKS	1402+044		1	3.202	18.50	-27.2	1.10	0	0		
	1409+0930	*	6	2.856	18.60	-27.5		0	0		
H	1413+117	*	2	2.546	17.00	-28.7	1.19	1	1	0.8	0.2
H	1413+117		5	2.546	17.00	-28.7	0.88	1	1	1.0	0.2
GB2	1413+373	*	3	2.360	18.00	-27.5	0.69	0	0		
Q	1414+0859	*	6	2.700	18.60	-27.3		0	0		
MAR	679	*	5	1.904	16.70	-28.6	0.84	0	0		
	1423+1007	*	1	2.775	18.40	-27.6	1.60	0	0		
Q	1426-0131	*	1	3.420	17.80	-28.0	1.00	0	0		
Q	1435-0134	*	1	1.310	16.00	-28.5	1.10	0	0		
OQ	172	*	4	3.530	17.78	-28.2	0.62	0	0		
PKS	1448-232	*	2	2.208	16.96	-28.4	0.92	0	1	0.0	0.0
PKS	1448-232		6	2.208	16.96	-28.4		0	0		
	1451+1223	*	6	3.256	18.60	-27.1		0	0		
	1455+1221	*	6	3.062	18.70	-27.3		0	0		
PKS	1502+106	*	1	1.833	18.56	-26.7	1.50	0	0		
B2	1506+33A	*	3	2.200	18.50	-26.9	0.74	0	0		
PKS	1508-05	*	1	1.191	17.21	-27.1	1.20	0	0		
LB	9612	*	5	1.901	17.28	-28.0	0.78	0	0		
MC	1517+176	*	1	1.402	17.50	-27.2	0.71	0	0		
SP	43		6	3.100	17.50	-28.4		0	0		
SP	43	*	3	3.100	17.50	-28.4	0.83	0	0		
PG	1522+101	*	2	1.321	15.65	-28.9	1.20	0	0		
PG	1522+101		6	1.321	15.65	-28.9		0	0		
	1548+0917	*	1	2.749	17.50	-28.5	0.72	0	0		
	1548+0917		5	2.749	17.50	-28.5	0.75	0	0		
	1548+0917		6	2.749	17.50	-28.5		0	0		
PKS	1551+130	*	4	1.290	17.65	-26.8	0.80	0	0		
GC	1556+33	*	5	1.646	17.00	-28.0	0.83	0	0		
GC	1556+33		3	1.646	17.00	-28.0	0.90	0	0		
PKS	1559+173	*	6	1.952	18.00	-27.3		0	0		
PKS	1559+173		4	1.944	18.00	-27.3	0.77	0	0		
TEX	1559+140		6	2.237	18.00	-27.4		0	0		
TEX	1559+140	*	4	2.237	18.00	-27.4	0.70	0	0		
B3	1621+392	*	6	1.970	17.50	-27.9		0	0		
	1623.7+268A		4	2.467	18.00	-27.5	1.07	0	0		
	1623.7+268A	*	3	2.400	18.00	-27.5	1.30	0	0		
	1623.7+268B		4	2.521	16.00	-29.6	0.77	0	0		
	1623.7+268B	*	3	2.518	16.00	-29.6	0.62	0	1	0.0	0.0
	1631.1+3738	*	3	2.940	18.60	-27.6	0.82	0	0		
B2	1633+38	*	4	1.814	18.00	-27.2	1.06	0	0		
MC	1634+176		6	1.897	18.00	-27.3		0	0		
MC	1634+176		4	1.897	18.00	-27.3	0.78	0	0		
MC	1634+176	*	3	1.897	18.00	-27.3	0.80	0	0		
	1635.5+26.6	*	1	1.950	20.50	-24.8	1.00	0	0		
S4	1656+47		4	1.622	18.00	-27.0	0.81	0	0		
S4	1656+47	*	3	1.622	18.00	-27.0	0.62	0	0		
1E	1704+710	*	6	2.000	17.50	-27.9		0	0		
IE	1711+712	*	6	1.600	17.50	-27.4		0	0		
PG	1715+535	*	3	1.920	16.50	-28.8	0.60	0	0		
PG	1715+535		5	1.929	16.48	-28.8	0.99	0	0		
PG	1718+481	*	6	1.084	14.71	-29.3		0	0		
B2	1722+33	*	3	1.870	18.00	-27.3	0.72	0	0		
	17449+206	*	3	2.410	19.00	-26.8	0.71	0	0		
WEE	167	*	3	2.430	19.80	-26.0	0.95	0	0		
PKS	1756+237	*	3	1.721	18.00	-27.1	0.52	0	0		
	1826.8+48.5	*	3	2.170	18.50	-26.9	0.70	0	0		
4C	56.28		6	1.595	17.30	-27.6		0	1	2.8	
4C	56.28	*	3	1.595	17.30	-27.6	0.68	0	1	2.9	2.6
PKS	1935-692	*	1	3.170	18.80	-27.0	1.30	0	0		
Q	1937-101	*	1	3.780	17.00	-29.2	0.90	0	0		
PKS	2000-330	*	2	3.777	19.00	-27.2	1.06	0	1	4.9	3.6
PKS	2020-370	*	1	1.048	17.46	-26.5	1.40	0	0		
PKS	2021-330	*	2	1.470	16.30	-28.5	1.13	0	0		
PKS	2021-330		6	1.470	16.30	-28.5		0	0		
	20374-007	*	3	2.300	19.90	-25.9	0.66	0	0		
	20382-012	*	3	2.900	19.10	-27.1	0.58	0	0		
Q	2038-371	*	1	3.000	18.53	-27.6	1.20	0	0		
Q	2040-374	*	2	2.276	17.84	-27.5	1.03	0	0		
Q	2040-374		6	2.276	17.84	-27.5		0	1	0.3	3.0
Q	2040-400	*	1	2.070	18.10	-27.4	1.10	0	0		
PKS	2044-168	*	2	1.943	17.36	-28.0	1.76	0	1	4.5	3.6
PKS	2047-655	*	2	2.320	17.50	-28.2	1.50	0	0		

TABLE 3. (continued)

Identification		F	Type	z	m	M	FWHM	PQ	OQ	θ_{DQ}	MQ
Q	2049-353	*	1	3.040	18.45	-27.6	1.10	0	0		
Q	2050-359	*	1	3.490	18.31	-27.6	1.30	0	0		
Q	2051-373	*	1	2.590	17.72	-28.0	1.20	0	0		
Q	2051-355	*	1	3.310	18.30	-27.4	1.10	0	0		
Q	2055-140	*	6	2.063	17.90	-27.6		0	0		
	2111.1+0629	*	3	2.330	19.80	-25.9	0.66	0	0		
Q	2112-407	*	1	2.543	18.00	-27.7	1.10	0	0		
PKS	2115-305	*	1	0.980	16.47	-27.3	1.20	0	1	3.0	2.0
Q	2116-358		2	2.341	17.35	-28.4	1.50	0	0		
Q	2116-358	*	6	2.341	17.35	-28.4		0	0		
	21189+168	*	3	2.300	19.50	-26.2	0.54	0	1	4.6	2.8
3C	432.0	*	3	1.805	18.00	-27.2	0.71	0	0		
PKS	2121+053		1	1.878	17.50	-27.8	0.81	0	0		
PKS	2121+053		6	1.878	17.50	-27.8		0	0		
PKS	2121+053		4	1.878	17.50	-27.8	1.05	0	0		
PKS	2121+053	*	3	1.878	17.50	-27.8	0.54	0	0		
Q	2123-408	*	1	2.290	18.50	-27.2	0.80	0	0		
Q	2125-1335	*	1	2.948	18.70	-27.5	0.90	0	0		
PKS	2126-15	*	2	3.275	17.30	-28.4	1.38	0	0		
PKS	2126-15		6	3.275	17.30	-28.4		0	0		
HA	2	*	1	2.093	17.55	-27.9	1.30	0	0		
PKS	2131+001	*	1	1.936	16.79	-28.5	0.68	0	0		
PKS	2131+001		5	1.936	16.79	-28.5	0.68	0	0		
PKS	2131+001		6	1.936	16.79	-28.5		0	0		
PKS	2131+004		3	1.936	16.80	-28.5	0.74	0	1	0.0	0.0
	21342-149	*	4	2.200	18.30	-27.1	0.69	0	0		
PKS	2136+141		6	2.427	18.50	-27.1		0	0		
PKS	2136+141	*	3	2.427	18.50	-27.1	0.48	0	0		
	21431+040	*	3	2.000	19.20	-26.2	0.66	0	0		
PKS	2144-362	*	6	2.081	17.80	-27.7		0	0		
PKS	2149-306	*	6	2.345	18.00	-27.7		0	0		
PKS	2150+05		6	1.979	17.77	-27.6		0	0		
PKS	2150+05		4	1.979	17.77	-27.6	0.67	0	0		
PKS	2150+05	*	3	1.979	17.80	-27.6	0.53	0	0		
PKS	2153-204	*	1	1.309	17.01	-27.5	0.65	0	0		
PKS	2153-204		6	1.309	17.01	-27.5		0	0		
B2	2156+29		6	1.753	17.50	-27.6		0	0		
B2	2156+29	*	3	1.753	17.50	-27.6	0.58	0	0		
	2158-214U	*	6	2.079	18.10	-27.4		0	0		
MC	2158+101	*	4	1.727	18.70	-26.4	0.77	0	0		
PB	5062	*	2	1.770	17.50	-27.7	1.13	0	0		
	2203+29	*	3	4.406	22.00	-24.5	0.57	0	0		
PKS	2204-573		2	2.725	17.36	-28.6	1.82	0	0		
PKS	2204-573	*	6	2.725	17.36	-28.6		0	0		
Q	2204-408		2	3.170	17.57	-28.2	2.09	0	0		
Q	2204-408	*	6	3.170	17.57	-28.2		0	0		
	2206-199N	*	1	2.559	17.33	-28.4	0.70	0	0		
	2209-187U		1	2.092	17.80	-27.7	1.36	0	0		
	2209-187U	*	6	2.092	17.80	-27.7		0	0		
PKS	2212-299	*	1	2.703	17.44	-28.5	0.69	0	0		
PKS	2212-299		6	2.703	17.44	-28.5		0	0		
Q	2219-394		1	2.022	17.74	-27.7	1.26	0	0		
Q	2219-394	*	6	2.022	17.74	-27.7		0	0		
PKS	2222+05	*	3	2.324	18.50	-27.2	0.75	0	0		
Q	2222-396	*	1	2.180	17.90	-27.5	0.65	0	0		
Q	2222-396		6	2.180	17.90	-27.5		0	0		
PKS	2223+21		6	1.959	18.00	-27.4		0	0		
PKS	2223+21	*	3	1.959	18.00	-27.4	1.00	0	0		
Q	2225-404	*	1	2.020	18.28	-27.1	0.70	0	0		
PHL	5200	*	2	1.981	17.70	-27.7	0.64	0	0		
PHL	5200		6	1.981	17.70	-27.7		0	0		
PHL	5200		4	1.981	17.70	-27.7	0.65	0	0		
PHL	5200		3	1.981	17.70	-27.7	0.65	0	0		
PKS	2227-08	*	1	1.562	17.50	-27.4	0.65	0	0		
PKS	2227-08		5	1.562	17.50	-27.4	0.72	0	0		
Q	2228-399	*	1	2.200	18.30	-27.1	0.81	0	0		
	2233.9+1318	*	3	3.280	18.20	-27.5	0.46	0	0		
	2237.9+0040	*	3	2.200	18.40	-27.0	0.72	0	0		
UM	657	*	1	1.360	17.20	-27.4	0.83	0	0		
UM	657		6	1.360	17.20	-27.4		0	0		
	2239.5+0073	*	3	2.400	19.80	-26.1	0.45	0	0		
Q	2240-419	*	6	2.080	18.00	-27.5		0	0		
Q	22409-3702	*	1	1.820	18.00	-27.2	0.69	0	0		
UM	658	*	6	2.850	18.10	-28.0		0	0		
PKS	2245-328	*	1	2.268	18.60	-26.8	1.10	0	0		
PKS	2246-309	*	1	1.307	17.00	-27.5	0.73	0	0		
Q	2246-389	*	2	2.120	17.90	-27.6	1.39	0	0		
Q	2246-389		6	2.120	17.90	-27.6		0	0		
4C	19.74	*	4	1.806	18.70	-26.5	0.80	0	0		
PKS	2251+24		5	2.328	17.80	-28.0	0.61	0	0		
PKS	2251+24		6	2.328	17.80	-28.0		0	0		
PKS	2251+24	*	3	2.328	17.80	-28.0	0.48	0	0		
PKS	2254+024		2	2.090	17.00	-28.5	1.53	0	0		
PKS	2254+024		5	2.089	17.00	-28.5	0.62	0	0		
PKS	2254+024		6	2.090	17.00	-28.5		0	0		
PKS	2254+024	*	3	2.090	17.00	-28.5	0.58	0	0		
PKS	2256+017		4	2.663	19.00	-26.8	0.63	0	0		
PKS	2256+017	*	3	2.663	19.00	-26.8	0.55	0	0		
Q	2258-391	*	6	2.050	18.00	-27.4		0	0		
Q	2300-352		2	2.840	17.90	-28.2	1.64	0	0		
Q	2300-352	*	6	2.840	17.90	-28.2		0	0		
PG	2302+029	*	1	1.044	16.10	-27.8	0.71	0	0		
PG	2302+029		6	1.044	16.10	-27.8		0	0		
TEX	2303+183	*	4	1.557	18.00	-26.9	0.63	0	0		
Q	2304-423	*	6	2.630	17.60	-28.2		0	0		
PKS	2319+07	*	4	2.090	18.50	-27.0	0.76	0	0		
UM	164		6	1.900	17.00	-28.3		0	0		
UM	164	*	3	1.900	17.00	-28.3	0.63	0	0		
	2333+019B		4	1.871	18.00	-27.3	0.87	0	0		
	2333+019B	*	3	1.871	18.00	-27.3	0.75	0	0		
PKS	2335-181	*	6	1.441	17.34	-27.4		0	0		
PKS	2335-181		1	1.441	17.34	-27.4	1.10	0	0		
PKS	2338+042	*	3	2.592	19.50	-26.2	0.94	0	0		
BG	CFH 26	*	3	2.140	19.70	-25.8	0.58	0	0		
BG	CFH 27	*	3	2.340	18.70	-27.0	0.61	0	0		
UM	660	*	6	2.822	18.10	-28.0		0	0		
UM	175		6	1.960	18.60	-26.8		0	0		
UM	175	*	3	1.960	18.00	-27.4	0.58	0	0		
BG	CFH 35	*	3	2.700	18.90	-27.0	0.48	0	0		
BG	CFH 44	*	3	2.100	19.80	-25.7	0.48	0	0		
UM	180	*	4	1.960	18.00	-27.4	0.87	0	0		
PKS	2345+061		6	1.546	17.50	-27.4		0	0		
PKS	2345+061	*	4	1.538	17.50	-27.4	0.67	0	0		
UM	184		6	3.005	19.50	-26.6		0	0		
UM	184	*	4	3.005	19.50	-26.6	0.62	0	0		
Q	2348-4025	*	1	3.310	18.60	-27.1	0.99	0	0		
Q	2348-4025		6	3.310	18.60	-27.1		0	0		
WEE	180	*	3	2.040	19.80	-25.6	0.67	0	0		
Q	2349-012	*	1	3.120	16.50	-29.3	1.00	0	0		
PKS	2351-154	*	2	2.665	17.00	-28.9	1.20	0	0		
PKS	2351-154		6	2.665	17.00	-28.9		0	0		
PKS	2352-455	*	2	1.868	17.50	-27.8	1.01	0	0		
PKS	2352-455		6	1.868	17.50	-27.8		0	0		
PKS	2353+154		4	1.801	18.00	-27.2	0.69	0	0		
PKS	2353+154	*	3	1.801	18.00	-27.2	0.63	0	0		
PKS	2354+14		4	1.810	18.18	-27.0	0.62	0	0		
PKS	2354+14	*	3	1.810	18.20	-27.0	0.42	0	0		
PKS	2354+14		1	1.810	18.18	-27.0	0.90	0	0		
Q	2355-025	*	1	2.050	17.50	-27.9	1.00	0	0		
Q	2355-389	*	6	2.850	18.40	-27.7		0	0		
PKS	2355-106	*	4	1.622	18.50	-26.5	1.13	0	0		
Q	2355-019	*	1	1.640	16.50	-28.5	1.00	0	1	1.9	3.0
Q	2355+019	*	1	2.790	17.50	-28.5	1.00	0	0		
UM	193	*	1	2.070	18.40	-27.1	1.21	0	0		
UM	193		4	2.070	18.40	-27.1	0.81	0	0		
Q	2357-348	*	1	2.070	17.78	-27.7	1.00	0	0		
Q	2357-348		6	2.070	17.78	-27.7		0	0		
PKS	2357-326	*	6	1.275	17.00	-27.5		0	0		
PKS	2358-161	*	6	2.044	18.00	-27.4		0	0		
	2359+0653	*	6	3.234	18.80	-26.9		0	0		
UM	196		4	2.817	18.70	-27.4	0.67	0	0		
UM	196		6	2.817	18.00	-28.1		0	0		
UM	196	*	3	2.820	18.00	-28.1	0.71	0	0		

Notes:

Col. 1: HLQ identification

Col. 2: An asterisk (*) in this column indicates which of the listed observation(s) for a same HLQ turned out to be the best one for calculating, in section 3, the effectiveness parameter F of galaxies to produce multiply lensed quasar images

Col. 3: Type as defined in Table 2

Col. 4: Redshift z of the HLQ

Col. 5: m is the apparent magnitude of the HLQs as listed under the column V in the catalogue of Véron-Cetty and Véron (1991). Unfortunately, these magnitudes are not always "visual" ones; they are generally quite inaccurate and inhomogeneous.

Col. 6: M stands for absolute visual magnitudes, calculated from the apparent magnitudes m (see Col. 5) and assuming H_0 = 50 km/sec/Mpc and q_0 = 0.5. Note that k-corrections were applied with α = -0.7 and a magnitude correction for the presence of broad emission lines (see Véron-Cetty and Véron 1991).

Col. 7: FWHM corresponds to the full width at half maximum, in arcsec., of stellar images recorded on the CCD frames.

Cols. 8 & 9: Indications on whether the HLQ consists of a confirmed GL (PQ = 1) or of just a possible candidate (OQ = 1, but PQ = 0, for such candidates).

Cols. 10 & 11: If PQ = 1 or OQ = 1, we list here the distance θ_{DQ} (in arcsec) and the magnitude difference MQ between the identified secondary point source image and the primary one. Null values in these columns indicate that the relevant quantities could not be determined satisfactorily (cf. the position of a faint residual obtained from a PSF subtraction).

(iv) when deriving the expression of τ, TOG assume that there is no evolution of the lens properties with cosmic time [i.e., $n(z) \propto n(0)(1+z)^3$]. Mao (1991) has shown that a simple redshift cutoff model for the lensing galaxies may significantly reduce the lensing probability and also explain the large mean separation of images for known lenses such as 0957+561, 2345+007, etc. Mao also warns that such an effect could mask the contribution of a non-negligible cosmological constant Λ in producing the apparent observed number of lenses,

(v) the above derivation of τ is only valid for the case of an isolated lens. Jaroszynski (1991) has shown numerically that the grouping of galaxies and possible correlations between galaxies and background matter density may increase the probability of high amplifications. Other possible intervening density inhomogeneities (cf. granularity in the galaxies, cluster substructure at kpc scales, etc.) could also be of some importance but were not taken into account because of lack of better knowledge;

(vi) probably of great importance is the inadequacy of the SIS model to account for the observed GL configurations which consist of more than two images, and thus it cannot be expected to give a very precise estimate of τ, neither of the magnification bias. Using an elliptical lens model with realistic physical parameters (core radius, ellipticity, etc.) and by means of extensive Monte-Carlo simulations, Kochanek (1991b) and Wallington & Narayan (1992) have recently proposed more accurate estimates of τ. It would certainly be very appropriate to apply in the future their formalism to the observational results compiled in the present paper;

(vii) Finally, it should be noted that the sensitivity of τ upon the redshift-distance formulation and statistics formalism has been investigated by FFKT. Based upon numerical simulations (provided that there are no sources at very large redshifts, i.e., $z_Q \leqslant 3$), they conclude that the formulation dependence is small in the final prediction of lenses. Note also that τ is independent of H_0 and also on the possible extra lensing brought by galaxy clusters since we did not consider GL candidates with image separations greater than $\simeq 3''$.

On account of part of the complications listed above, Kochanek (1991b) has estimated that the error affecting the optical depth τ for lensing should be of the order of at least a factor 4.

We therefore conclude that our results on the expected number $N^{\exp}$ of GLs (cf. Table 4) agree sufficiently well with current expectations (cf. FT) and that it is not justified at the present time to compare observed to estimated numbers of multiply imaged quasars in order to infer the values of cosmological parameters such as Λ, Ω_0, etc.

3.2 Compact Lenses

3.2.1 The method

Press & Gunn (1973) have pointed out that the frequency of lensing events caused by a population of compact objects measures their contribution Ω_L to Ω_0, Ω_L being the local density of lensing points in units of the critical

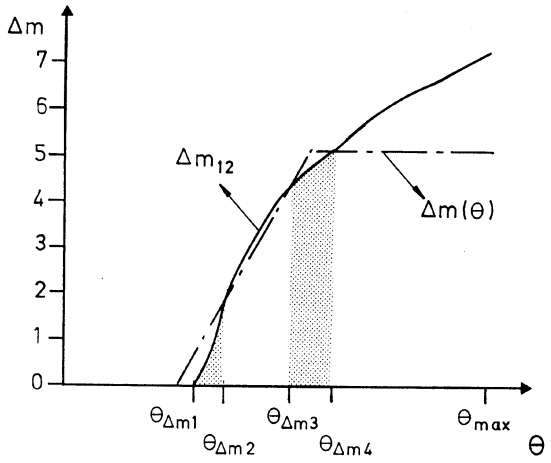

FIG. 3. One example of possible multiple intersections ($\theta_{\Delta mi}$, with generally $i \leqslant 4$) between the "angular selection function" $\Delta m(\theta)$ (cf. Fig. 2) and the predicted magnitude difference Δm_{12} between the two lensed images of a distant quasar. Note that $\theta_{\Delta m1} = 2\theta_E$, where θ_E represents the angular radius of the Einstein ring associated with the compact lens. $\theta_{\max}$ ($=3''$) is the maximum angular radius of the field under consideration (see text).

density. Adopting the "detection volume" formalism developed by Nemiroff (1991a,b) and Kassiola *et al.* (1991) in order to derive an expression for the lensing optical depth τ_Q of a distant quasar by a hypothetical population of compact lenses in the Universe, with mass $\mathcal{M}_L$, it is easy to establish that

$$\tau_Q = \pi \int_0^{D^P_{OQ}} n(D^P_{OL}) [\mathrm{Min}(b^2_{\Delta m2}, b^2_{\max}) - \mathrm{Min}(b^2_{\Delta m1}, b^2_{\max}) + \mathrm{Min}(b^2_{\Delta m4}, b^2_{\max}) - \mathrm{Min}(b^2_{\Delta m3}, b^2_{\max})] dD^P_{OL}, \quad (9)$$

$\tau_Q (\ll 1)$ representing in fact the expected number of lenses, distributed with a cosmic density $n(z_L) = n_0(1+z_L)^3$ at a proper distance D^P_{OL} from the observer, inside a volume such that they are capable of producing observable double images of a distant quasar Q. In the above expression for τ_Q, several observational biases are implicitly taken into account. For instance, we have constrained the lensed images to be characterized by a magnitude difference smaller than Δm, which is itself a function of θ (cf. Fig. 2, see also the Δm–θ relations given in Table 2) and by a maximum angular separation $\theta_{\max}$ (set to $3''$ in our calculations). In the above equation, the quantities $b_{\Delta mi}$ ($i=1$–4) and $b_{\max}$ represent extreme impact parameters defined in the lens plane such that $b_{\Delta mi} = D_{OL}\theta_{\Delta mi}$ (respectively, $b_{\max} = D_{OL}\theta_{\max}$), where D_{OL} is the angular distance of the lens as measured by the observer and where the $\theta_{\Delta mi}$ ($i=1$–4, respectively $\theta_{\max}$) represent possible intersecting points between the Δm–θ function (cf. Fig. 2) and the expected magnitude difference Δm_{12} between the two lensed images 1 and 2 of a distant quasar (see Fig. 3). The values of the impact parameters $b_{\Delta mi}$ ($i=1$–4) and $b_{\max}$ also depend on the angular distances D_{OQ}, D_{OL}, and D_{LQ} between the observer O, the quasar Q and the lens L; they are easily derived numerically in the framework of the point mass

TABLE 4. Results on F and $N^{\exp}$ from our statistical GL studies (see text).

Ω_0	λ_0	$F_{\rm lo}(99.7\%)$	$F_{\rm up}(99.7\%)$	$N^{\exp}_{\rm lo}$	$N^{\exp}_{\rm up}$
1	0	0.005	0.478	1.3	2.6
0.1	0.9	0.001	0.090	6.7	13.7
0	1	0.0004	0.037	16.7	33.4
0	0	0.003	0.265	2.3	4.7

lens model (cf. Claeskens 1992; see also Nemiroff 1991a, b and Kassiola *et al.* 1991).

One may then write the relation between the effective optical depth τ for the lensing of N_Q quasars by a cosmic population of compact lenses, with mass $\mathcal{M}_L$ and density parameter Ω_L, as follows:

$$\tau = N_L/N_Q = \Omega_L \sum_{q=1}^{N_Q} G(z_q, b_q, \text{Type}, \theta_{\max}, \mathcal{M}_L, \Omega_L) S_{\rm cat}/N_Q , \quad (10)$$

where most of the quantities have been defined in Sec. *3.1* [cf. Eq. (1)] and where

$$G(z_q, b_q, \text{Type}, \theta_{\max}, \mathcal{M}_L, \Omega_L) = \frac{3H_0 c}{8G\mathcal{M}_L} \cdot \int_0^{z_q} \frac{(1+z)}{\sqrt{1+\Omega_0 z}} [[\text{Min}(b^2_{\Delta m2}, b^2_{\max}) - \text{Min}(b^2_{\Delta m1}, b^2_{\max})] B(b_q, \Delta_{\min}) + [\text{Min}(b^2_{\Delta m4}, b^2_{\max}) - \text{Min}(b^2_{\Delta m3}, b^2_{\max})] \times B(b_q, \Delta_{\min})] dz. \quad (11)$$

In the above expression, the magnification bias $B(b_q, \Delta_{\min})$ is calculated by means of Eq. (5) adopting the compact lens (CL) point source amplification probability

$$P_{\rm CL}(\Delta) = \frac{e^{\Delta/1.086}(e^{2\Delta/1.086}-1)^{-1.5}}{1.086[0.5(10^{(\Delta m_{i/i+1})/5} + 10^{-(\Delta m_{i/i+1})/5}) - 1]}, \quad (12)$$

with

$$\Delta_{\min} = 2.5 \log\left[\frac{10^{(\Delta m_{i/i+1})/2.5}+1}{10^{(\Delta m_{i/i+1})/2.5}-1}\right], \quad (13)$$

where $\Delta m_{i/i+1}$ (for $i=1$ or $i=3$) represents a typical value of the ASF between the intersecting solutions $\theta_{\Delta mi}$ and $\theta_{\Delta mi+1}$ (see Fig. 3). Let us note that, in Eq. (11), G appears to be a function of Ω_L because of the slight dependence of the Dyer–Roeder angular distance D_{LQ} on Ω_L (Dyer & Roeder 1973). In practice, Eq. (11) is successfully solved numerically by means of a Gauss–Legendre method with 9 points.

3.2.2 Numerical applications and results

Making use of the 469 quasars observed within the ESO-KP, Crampton *et al.*, Yee *et al.*, and *HST* snapshot samples, we have applied Eqs. (10)–(13) in order to set upper limits on the parameter Ω_L for compact lenses in the mass range 10^{10}–$10^{12}\mathcal{M}_\odot$ (see Table 5). With a 99.7% confidence level and adopting $H_0=50$ km/s/Mpc, $\Omega_0=1$ and $\Lambda=0$, we find that $\Omega_L \leqslant 0.02$; it is even likely that $\Omega_L \ll 0.02$ (if none of the known GL systems is due to a compact deflector).

TABLE 5. Results on Ω_L from our statistical GL studies (see text).

Ω_0	λ_0	$\Omega_L^{\rm sup}(99.7\%)$	$\mathcal{M}_L(\mathcal{M}_\odot)$
1	0	0.057	10^{10}
1	0	0.021	5×10^{10}
1	0	0.018	10^{11}
1	0	0.028	5×10^{11}
1	0	0.059	10^{12}
0.1	0.9	0.005	10^{11}
0.0	1.0	0.003	10^{11}
0.0	0.0	0.012	10^{11}

3.2.3 Discussion

In 1982, Canizares used the small observed variation in the equivalent widths of broad emission lines recorded in the spectrum of quasars to exclude a closure density of compact objects in the range $10^{-2} \leqslant \mathcal{M}_L/\mathcal{M}_\odot \leqslant 10^5$.

From the number of multiply imaged radio sources detected in the VLA lens survey, Hewitt (1986) could derive,under reasonable assumptions, $\Omega_L < 0.4$ for compact objects in the mass range 10^{11}–$10^{13}\mathcal{M}_\odot$.

Using the results reported by Crampton *et al.* (1989) for the number of possible GL candidates identified in a sample of HLQs (see Sec. *2.2*), Nemiroff (1991a) has applied his "detection volume formalism" to deduce that $\Omega_L < 1$ (respectively, $\Omega_L < 0.25$) for compact objects having a mass $\mathcal{M}_L > 10^{9.9}\mathcal{M}_\odot$ (respectively, $\mathcal{M}_L > 10^{10.3}\mathcal{M}_\odot$). Note, however, that Nemiroff did not include in his calculations the—important—magnification bias correction factor, discussed previously.

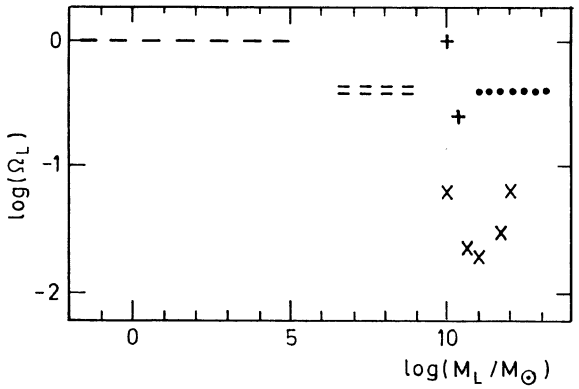

FIG. 4. Adopting $H_0=50$ km/s/Mpc, $\Omega_0=1$ and $\Lambda=0$, we have illustrated in this diagram the various upper bounds derived for the density parameter Ω_L of compact lenses, with mass $\mathcal{M}_L$, capable of producing multiple images of distant sources. The various determinations are from (–) Canizares (1982), (.) Hewitt (1986), (+) Nemiroff (1991a), (=) Kassiola *et al.* (1991) and (×) the present work.

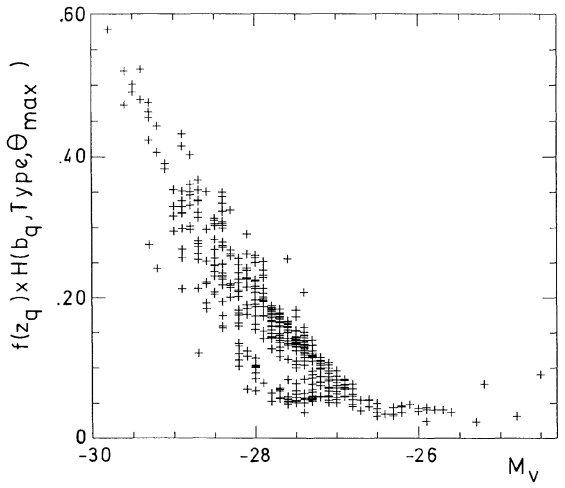

FIG. 5. The quantity $f(z_q)H(b_q,\text{Type},\theta_{\max})$ is represented as a function of the absolute magnitude M_V for each of the 469 HLQs observed in the merged sample.

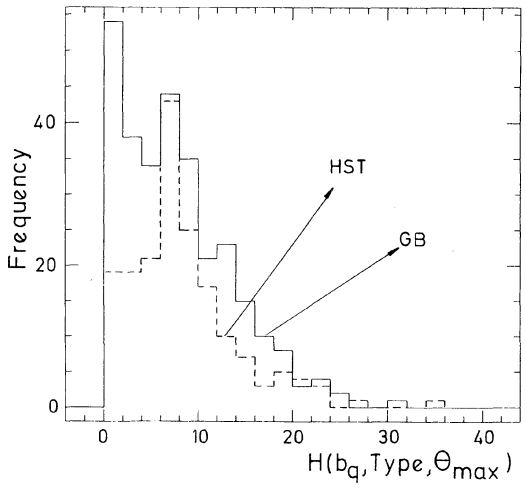

FIG. 6. Histogram of the function $H(b_q,\text{Type},\theta_{\max})$ [see Eqs. (6) and (7)] for the 659 observations of HLQs either obtained with ground based (GB) telescopes or with *HST*.

Kassiola *et al.* (1991) have investigated the constraints that can be imposed on the cosmic density of uniformly distributed intergalactic compact objects in the range $10^7 \leqslant \mathcal{M}_L/\mathcal{M}_\odot \leqslant 10^9$ using VLBI observations of compact radio sources. They exclude $\Omega_L > 0.4$ at the 99.7% confidence level.

We have summarized in Fig. 4 all previous estimates quoted for Ω_L over a wide range of deflector masses. It is striking that the cosmological density of compact objects in the mass range 10^{10}–10^{12} $\mathcal{M}_\odot$ is presently the best constrained one: it already appears to be much lower than that of known galaxies!

4. DISCUSSION

4.1 Quasars Multiply Imaged by Singular Isothermal Sphere (SIS) Galaxies

Considering first the astronomical aspect of gravitational lensing, it is obvious from Eq. (6) that in order to maximize the detection of GL systems among HLQs, one should select quasars such that the quantity $f(z_q)H(b_q,\text{Type},\theta_{\max})$ is as large as possible. We have represented in Fig. 5, for each of the 469 HLQs belonging to the merged sample, this quantity as a function of the absolute magnitude M_V. The correlation existing between the quantity $f(z_q)H(b_q,\text{Type},\theta_{\max})$ and M_V clearly shows why selecting a sample of quasars with an intrinsic brightness as high as possible constitutes the best approach to search for new lenses as well as to constrain most efficiently the value of the effectiveness parameter F.

Addressing now the observational strategy to follow when searching for new GLs, we see from Eq. (6) that the function $H(b_q,\text{Type},\theta_{\max})$ should also be maximized with respect to the ASF, i.e., one should make use of the instruments characterized by the best resolving power (e.g., under optimal seeing conditions for the ground based observations) with as large a dynamical range as possible. We have illustrated in Fig. 6 the histogram of that quantity for the 659 observations of the 469 HLQs available so far, in accordance with the "angular selection functions" given in Table 2 (see also Fig. 2). Although the angular resolution of the *HST* observations is substantially superior to that of the ground based data, the corresponding dynamical range is presently more limited, resulting in a very comparable efficiency for the detection of GL candidates. Given the lower costs of operating instruments from the ground, there is no doubt that observations of HLQs obtained with a 2–4 m ground based telescope and characterized by a large dynamical range ($\Delta m \geqslant 5$ mag) and high angular resolution (optimal seeing conditions or using a speckle camera) should provide in the near future the best strategy to search for new GLs.

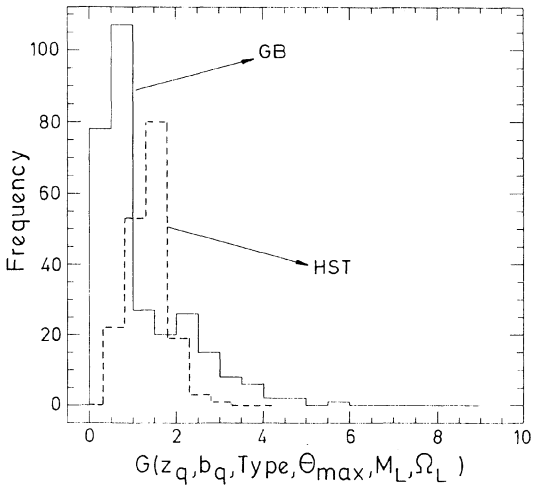

FIG. 7. Histogram of the quantity $G(z_q,b_q,\text{Type},\theta_{\max},\mathcal{M}_L,\Omega_L)$ [see Eqs. (10) and (11)] for the 659 observations of HLQs either obtained with ground based (GB) telescopes or with *HST* ($\mathcal{M}_L = 10^{10}\mathcal{M}_\odot$).

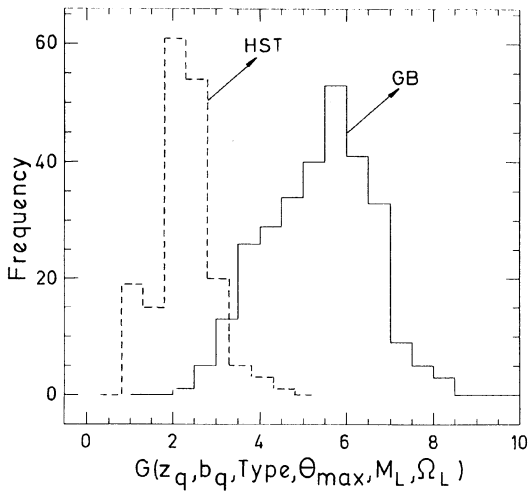

FIG. 8. Histogram of the quantity $G(z_q,b_q,\text{Type},\theta_{\max},\mathcal{M}_L,\Omega_L)$ [see Eqs. (10) and (11)] for the 659 observations of HLQs either obtained with ground based (GB) telescopes or with *HST* ($\mathcal{M}_L=10^{11}\mathcal{M}_\odot$).

4.2 Quasars Multiply Imaged by Compact Objects

We have represented in Figs. 7 and 8 the histograms of the quantity $G(z_q,b_q,\text{Type},\theta_{\max},\mathcal{M}_L,\Omega_L)$ appearing in Eqs. (10)–(11) for $\mathcal{M}_L=10^{10}$ and $\mathcal{M}_L=10^{11}\mathcal{M}_\odot$, respectively. We conclude here also that the efficiency of ground based instruments used to constrain the values of the density parameter Ω_L in the mass range 5×10^{10}–$10^{12}\mathcal{M}_\odot$ appears to be as good as that of *HST*. Note that only for $\mathcal{M}_L\leqslant5\times10^{10}\mathcal{M}_\odot$, does the efficiency of *HST* become superior to that of ground based observations. Replacement of the WFPC I camera by WFPC II should, of course, improve much the efficiency of future *HST* observations.

5. GENERAL CONCLUSIONS

Generally speaking, gravitational lensing effects may alter the observed number counts of distant quasars in various ways. Whereas we have considered in this work the phenomenon of multiply imaged quasars at $\simeq0.1''$–$3''$ angular scales, it should be noted that magnification of distant quasars may also result from microlensing effects due to stellar and/or planetarylike objects in intervening galaxies as well as by matter (galaxies, clusters, large sheets of dust and gas, other—unknown?—forms of dark matter, etc.) at various possible locations along the line-of-sight.

In the present paper, we have applied statistical gravitational lens studies to a sample of 469 highly luminous quasars (HLQs), either observed from the ground or with *HST*, in order to estimate the effectiveness parameter F of singular isothermal sphere (SIS) galaxies as well as upper bounds on the density parameter Ω_L of compact objects in the mass range 10^{10}–$10^{12}\mathcal{M}_\odot$. For the values of the cosmological parameters $H_0=50$ km/s/Mpc, $\Omega_0=1$ and $\Lambda=0$, we have found at a significance level of 99.7% that (i) $0.005<F<0.478$, a result which overlaps current expectations (FT) and that (ii) $\Omega_L\leqslant0.02$, implying that less than 2% of the closure density of the Universe is in the form of compact objects with masses in the range $10^{10}\leqslant\mathcal{M}_L/\mathcal{M}_\odot\leqslant10^{12}$.

We have reviewed in Sec. *3.1.3* all the types of uncertainties which may affect the previous estimates of F, and we have concluded that it is presently hazardous to use the observed fraction of multiply lensed quasars in order to derive an estimate of the cosmological parameter Λ. Note that our estimated upper bounds on Ω_L also strongly depend on the adopted value for Λ (see Table 5 and FFK).

In Sec. 4, we have compared the efficiencies of ground based and of *HST* observations carried out for the 469 selected HLQs in a search for new lenses. We have concluded that these efficiencies were presently very comparable (cf. Sec. *4.2*). Furthermore, because of the present difficulties related to the spherical aberration of *HST*, to the variation of the PSF over the field of the WF/PC camera, etc. and due to a significant difference in operational costs, we have argued that obtaining direct imagery of HLQs, with a 2–4 m class ground based telescope equipped with an optical speckle camera or working under very good seeing conditions, still constitutes the best approach to search for multiply lensed quasars. Observing a medium size sample of HLQs with a speckle camera characterized by a dynamical range $\Delta m=5$ mag would allow one to constrain the density parameter Ω_L to less than 0.01 in the mass range 10^8–10^{10} $\mathcal{M}_\odot$, a search for massive compact objects near $10^9\mathcal{M}_\odot$ being of course dictated by the possible existence of dark black holes with masses similar to AGN central engines. Note that quite a number of HLQs observed with *HST* show possible structures at $0.1''$–$0.2''$ scales (cf. Maoz *et al.* 1992b); however, because of the complex PSF shape, it is not possible to conclude at present whether these structures are real or due to PSF artifacts.

As may be seen from Fig. 4, much work has still to be done in order to improve the constraints on Ω_L for compact objects in the mass range 10^{-8}–$10^{10}\mathcal{M}_\odot$. It is likely that novel techniques will be developed and applied in the near future. For instance, Refsdal (1990) has suggested to use simultaneous observations of remote quasars from the Earth and from a distant spacecraft in order to search for lensing effects by compact lenses in the mass range 10^{-8}–10^4 $\mathcal{M}_\odot$. Kassiola *et al.* (1991) have predicted that using the capabilities of the VLBA ($\theta_{\text{res}}=0.0005''$, dynamical range $R=1000$), future observations should allow one to exclude or discover $\Omega_L\geqslant10^{-3}$ for compact objects in the range $10^5\leqslant\mathcal{M}_L/\mathcal{M}_\odot\leqslant10^8$. The optical interferometric mode of future Very Large Telescopes (e.g., the ESO VLT) should also allow one to probe quite soon the mass range 10^6–$10^8\mathcal{M}_\odot$ for hypothetical compact objects.

In the context of observational searches for massive astrophysical compact objects located in the halo of our Galaxy (MACHOs, cf. Paczynski 1986), let us mention that ongoing projects should lead to the possibility of exploring the presence of compact deflectors in the mass range 10^{-8}–$10^{-1}\mathcal{M}_\odot$, including brown dwarf and planet candidates (Bennett *et al.* 1991; Alcock *et al.* 1992; Vidal-Madjar *et al.* 1992; etc.).

J. S. wishes to thank Chris Kochanek for having encouraged us to publish the present data and results. Our thanks go also to Jean-Pierre Swings and Philippe Véron for reading the manuscript and for their comments, and to Armand Kransvelt for the preparation of the figures. Part of this research has been supported by Contract No. ARC 90/94-140 "Action de Recherche Concertée de la Communauté Française" (Belgium) and a FNRS grant (D.H.). A.V.F. acknowledges the support of NSF Grant No. AST-8957063.

REFERENCES

Alcock, C., *et al.* 1992, in the Proceedings of the Hamburg Conference on Gravitational Lenses, Lecture Notes in Physics 406, 156, edited by R. Kayser, T. Schramm, and L. Nieser (Springer, Berlin)
Bahcall, J. N., Maoz, D., Doxsey, R., Schneider, D. P., Bahcall, N. A., Lahav, O., & Yanny, B. 1992a, ApJ, 387, 56
Bahcall, J. N., Maoz, D., Schneider, D. P., Yanny, B., & Doxsey, R. 1992b, ApJ, 392, L1
Bennett, D. P., *et al.* 1991, preprint
Blandford, R. D., & Narayan, R. 1992, ARA&A, 30, 311
Boyle, B. J., Shanks, T., & Peterson, B. A. 1988, MNRAS, 235, 935
Canizares, C. R. 1982, ApJ, 263, 508
Claeskens, J. F. 1992, Master thesis, Liège University
Crampton, D., McClure, R. D., Fletcher, J. M., & Hutchings, J. B. 1989, AJ, 98, 1188
Crampton, D., McClure, R. D., & Fletcher, J. M. 1992, preprint
Djorgovski, S., Perley, R., Meylan, G., & McCarthy, P. 1987, ApJ, 321, L17
Djorgovski, S., & Meylan, G. 1989a, in Active Galactic Nuclei, IAU Symposium No. 134, edited by D. Osterbrock and J. Miller (Kluwer, Dordrecht), p. 269
Djorgovski, S., & Meylan, G. 1989b, in Gravitational Lenses, edited by J. M. Moran *et al.* (Springer, New York), p. 173
Dyer, C. C., & Roeder, R. C. 1973, ApJ, 180, L31
Fukugita, M., & Turner, E. L. 1991, MNRAS, 253, 99 (FT)
Fukugita, M., Futamase, T., & Kasai, M. 1990, MNRAS, 246, 24P (FFK)
Fukugita, M., Futamase, T., Kasai, M., & Turner, E. L. 1992, ApJ, 393, 3
Hartwick, F. D. A., & Schade, D. 1990, ARA&A, 28, 437
Hewitt, J. N. 1986, Ph.D. thesis, MIT
Jaroszynski, M. 1991, MNRAS, 249, 430
Kassiola, A., Kovner, I., & Blandford, R. 1991, ApJ, 381, 6
Kochanek, C. 1991a, private communication
Kochanek, C. S. 1991b, ApJ, 379, 517
Kochanek, C. S. 1991c, preprint
Magain, P., Surdej, J., Swings, J. P., Borgeest, U., Kayser, R., Kühr, H., Refsdal, S., & Remy, M. 1988, Nature, 334, 325
Magain, P., Remy, M., Surdej, J., Swings, J. P., & Smette, A. 1990, in Lecture Notes in Physics, Gravitational Lensing, Proceedings of the Toulouse Workshop on Gravitational Lenses, September 1989, edited by Y. Mellier, B. Fort, and G. Soucail (Springer, Berlin), Vol. 360, 88
Magain, P., Hutsemékers, D., Surdej, J., & Van Drom, E. 1992a, in the Proceedings of the Hamburg Conference on Gravitational Lenses, Lecture Notes in Physics 406, edited by R. Kayser, T. Schramm, and L. Nieser (Springer, Berlin), p. 88
Magain, P., Surdej, J., Vanderriest, C., Pirenne, B., & Hutsemékers, D. 1992b, A&A, 253, L13
Mao, S. 1991, ApJ, 380, 9
Maoz, D., *et al.* 1992a, ApJ, 386, L1
Maoz D., Bahcall, J. N., Doxsey, R., Schneider, D. P., Bahcall, N. A., Lahav, O., & Yanny, B. 1992b, preprint
Meylan, G., & Djorgovski, S. 1989, ApJ, 338, L1
Narayan, R. 1989, ApJ, 339, L53
Nemiroff, R. J. 1989, ApJ, 341, 579
Nemiroff, R. 1991a, Phys. Rev. Lett., 66, 538
Nemiroff, R. 1991b, Comments Astrophys., 15, 139
Paczynski, B. 1986, ApJ, 304, 1
Pirenne, B., Surdej, J., & Magain, P. 1992, ST-ECF Newsletter 17, 22
Press, W. H., & Gunn, J. E. 1973, ApJ, 185, 397
Refsdal, S. 1990, review paper in Lecture Notes in Physics, Gravitational Lensing, Proceedings of the Toulouse Workshop on Gravitational Lenses, September 1989, edited by Y. Mellier, B. Fort, and G. Soucail (Springer, Berlin), Vol. 360, p. 13
Schneider, P. 1991, MPA preprint 584
Surdej, J., *et al.* 1987, Nature 329, 695
Surdej, J., *et al.* 1988a, A&A, 198, 49
Surdej, J., Magain, P., Swings, J. P., Remy, M., Borgeest, U., Kayser, R., Refsdal, S., & Kühr, H. 1988b, invited paper to the First D.A.E.C. workshop on Large Scale Structures, proceedings edited by C. Balkowski and S. Gordon, p. 95
Surdej, J., *et al.* 1988c, Astron. Soc. of the Pac. Conf. Series 2, 183
Surdej, J., *et al.* 1989, The Messenger, 55, 8
Surdej, J. 1990, review paper in Lecture Notes in Physics, Gravitational Lensing, Proceedings of the Toulouse Workshop on Gravitational Lenses, September 1989, edited by Y. Mellier, B. Fort, and G. Soucail (Springer, Berlin), Vol. 360, pp. 57, 311
Surdej, J., *et al.* 1992a, invited paper to the Second D.A.E.C. meeting on the Distribution of Matter in the Universe, edited by G. A. Mamon and D. Gerbal, p. 97
Surdej, J., Claeskens, J. F., Hutsemékers, D., Magain, P., & Pirenne, B. 1992b, in the Proceedings of the Hamburg Conference on Gravitational Lenses, Lecture Notes in Physics 406, edited by R. Kayser, T. Schramm, and L. Nieser (Springer, Berlin), p. 27
Surdej, J. *et al.* 1993, in preparation
Swings, J. P., Magain, P., Remy, M., Surdej, J., Smette, A., Hutsemékers, D., & Van Drom, E. 1990, in Lecture Notes in Physics, Gravitational Lensing, Proceedings of the Toulouse Workshop on Gravitational Lenses, September 1989, edited by Y. Mellier, B. Fort, and G. Soucail (Springer, Berlin), Vol. 360, p. 83
Turner, E. L. 1990, ApJ, 365, L43
Turner, E. L., Ostriker, J. P., & Gott III, J. R. 1984, ApJ, 284, 1 (TOG)
Van Drom, E. 1992, in the Proceedings of the Hamburg Conference on Gravitational Lenses, Lecture Notes in Physics 406, edited by R. Kayser, T. Schramm, and L. Nieser (Springer, Berlin), p. 250
Van Drom, E., Surdej, J., Hutsemékers, D., Magain, P., Gosset, E., Shaver, P., & Melnick, J. 1993, A&A (submitted)
Véron-Cetty, M. P., & Véron, P. 1987, ESO Scientific Report No. 5
Véron-Cetty, M. P., & Véron, P. 1991, ESO Scientific Report No. 10
Vidal-Madjar, A., Aubourg, E., Kunth, D., Ferlet, R., & Mochkovitch, R. *et al.* 1992, invited paper to the Second D.A.E.C. Workshop on Large Scale Structures in the Universe (in press)
Wallington, S., & Narayan, R. 1992, preprint
Weymann, R. J., Latham, D., Angel, J. R. P., Green, R. F., Liebert, J. W., Turnshek, D. A., Turnshek, D. E., & Tyson, J. A. 1980, Nature 285, 641
Yee, H. K. C., Filippenko, A. V., & Tang, D. 1993, AJ, 105, 7